

# Online Research @ Cardiff

This is an Open Access document downloaded from ORCA, Cardiff University's institutional repository: <https://orca.cardiff.ac.uk/id/eprint/111906/>

This is the author's version of a work that was submitted to / accepted for publication.

Citation for final published version:

Raby, Anne-Catherine ORCID: <https://orcid.org/0000-0002-5354-5835>, González-Mateo, Guadalupe T., Williams, Aled, Topley, Nicholas, Fraser, Donald ORCID: <https://orcid.org/0000-0003-0102-9342>, López-Cabrera, Manuel and Labeta, Mario O. ORCID: <https://orcid.org/0000-0001-5750-6983> 2018. Targeting toll-like receptors with soluble toll-like receptor 2 prevents peritoneal dialysis solution-induced fibrosis. *Kidney International* 94 (2) , pp. 346-362. 10.1016/j.kint.2018.03.014 file

Publishers page: <http://dx.doi.org/10.1016/j.kint.2018.03.014>  
<<http://dx.doi.org/10.1016/j.kint.2018.03.014>>

Please note:

Changes made as a result of publishing processes such as copy-editing, formatting and page numbers may not be reflected in this version. For the definitive version of this publication, please refer to the published source. You are advised to consult the publisher's version if you wish to cite this paper.

This version is being made available in accordance with publisher policies.

See

<http://orca.cf.ac.uk/policies.html> for usage policies. Copyright and moral rights for publications made available in ORCA are retained by the copyright holders.



**Title: Targeting Toll-Like Receptors with Soluble Toll-Like Receptor 2 Prevents  
Peritoneal Dialysis Solution-Induced Fibrosis**

**Authors:** Anne-Catherine Raby<sup>1</sup>, Guadalupe T. González-Mateo<sup>2</sup>, Aled Williams<sup>1</sup>, Nicholas Topley<sup>1</sup>, Donald Fraser<sup>1</sup>, Manuel López-Cabrera<sup>2</sup> and Mario O. Labéta<sup>1</sup>

**Affiliations:** <sup>1</sup>Division of Infection & Immunity and The Wales Kidney Research Unit, School of Medicine, Cardiff University, Cardiff, United Kingdom; <sup>2</sup>Centro de Biología Molecular Severo Ochoa, CSIC-UAM, Cantoblanco, Madrid, Spain.

**Correspondence:** Anne-Catherine Raby or Mario O. Labéta, Division of Infection & Immunity, School of Medicine, Cardiff University, Tenovus Building, Heath Park, Cardiff, CF14 4XN, United Kingdom. E-mail: [RabyA@cardiff.ac.uk](mailto:RabyA@cardiff.ac.uk); phone: +44(0)2920687324; fax: +44 (0)29206 87303 or [wmdmol@cardiff.ac.uk](mailto:wmdmol@cardiff.ac.uk); phone: +44(0)2920687019; fax: +44 (0)29206 87303.

**Funding:** This work was funded by the Kidney Research UK (KRUK, Fellowship to A.-C.R.); Health and Care Research Wales (The Wales Kidney Research Unit); the ‘Ministerio de Economía y Competitividad’/Fondo Europeo de Desarrollo Regional (MINECO/FEDER; grant SAF2016-80648R to M.L.C) and the ‘Comunidad Autónoma de Madrid’ (FIBROTEAM Consortium; grant S2010/BMD-2321 to M.L.C).

**Running Title:** Preventing fibrosis in non-infected PD patients

## ABSTRACT

Peritoneal membrane failure due to fibrosis limits the use of peritoneal dialysis (PD). Peritoneal fibrosis may be induced by sterile inflammation caused by ongoing cellular stress induced by prolonged exposure to PD solutions (PDS). Effective therapies to prevent this process remain to be developed. Toll-like receptors (TLRs) mediate sterile inflammation by recognising damage-associated molecular patterns (DAMPs) released by cellular stress. We evaluated the involvement of TLRs and DAMPs in PDS-induced fibrosis and the therapeutic potential of TLR-DAMP targeting for fibrosis prevention. A range of PDS elicited pro-inflammatory and fibrotic responses (genes and proteins) from primary human uremic peritoneal leukocytes, mesothelial cells and mouse peritoneal leukocytes. TLR2/4 blockade in human peritoneal cells or TLR2/4 knockout inhibited these effects. PDS did not induce rapid ERK phosphorylation or I $\kappa$ B- $\alpha$  degradation, suggesting that they do not contain components capable of direct TLR activation. However, PDS increased the release of Hsp70 and hyaluronan - both TLR2/4 DAMP ligands - by human and mouse peritoneal cells and their blockade repressed PDS-driven inflammation. Soluble TLR2 (sTLR2), a TLR inhibitor, reduced PDS-induced pro-inflammatory and fibrotic cytokine release *ex vivo*. Daily catheter infusion of PDS in mice led to robust peritoneal fibrosis. Co-administration of sTLR2, however, prevented fibrosis development, suppressing pro-fibrotic gene expression, pro-inflammatory cytokine production, reducing leukocyte/neutrophil recruitment, recovering Treg cell levels and increasing the Treg:Th17 ratio. The study reveals a major role of TLR2/4, Hsp70 and hyaluronan in PDS-induced peritoneal inflammation and fibrosis and demonstrates the therapeutic potential of a TLR-DAMP targeting strategy to prevent PDS-induced fibrosis.

**Keywords:** PD; fibrosis; inflammation; peritoneal membrane

## INTRODUCTION

The success of peritoneal dialysis (PD) as a therapy depends on maintaining the structural and functional integrity of the peritoneal membrane. A major factor limiting the long-term use of PD remains peritoneal membrane failure, which is directly related to the progressive thickening of the sub-mesothelial compact zone, termed fibrosis, resulting in altered solute transport and dialysis failure. Fibrosis is driven by peritoneal inflammation, caused by recurrent infections and/or by ongoing cellular stress and tissue injury induced by the dialysis process (sterile inflammation).<sup>1</sup> The mechanisms linking inflammation – either infection-induced or sterile – with the genesis and regulation of fibrosis are the focus of intense investigation.<sup>2, 3</sup>

Prolonged exposure to PD solutions (PDS), particularly to those bio-incompatible (low pH and high glucose concentration), the concomitant formation of glucose degradation products and generation of advanced glycation end-products as well as uraemia and the presence of a catheter have all been reported to induce cellular stress and tissue injury resulting in sterile peritoneal inflammation. This in turn leads to local angiogenesis, vasculopathy, epithelial-to-mesenchymal transition in mesothelial cells, collagen deposition in the sub-mesothelial compact zone and subsequent peritoneal fibrosis and membrane failure.<sup>1, 4-6</sup> The immune mechanisms underlying sterile peritoneal inflammation resulting from prolonged exposure to PDS and leading to fibrosis development are poorly defined. Consequently, effective therapies to prevent PDS-associated fibrosis remain to be developed.

Cellular stress and tissue damage lead to the release of endogenous cellular components and to the generation of extracellular matrix degradation products which act as damage-associated molecular patterns (DAMPs), triggering pro-inflammatory and pro-fibrotic responses.<sup>7</sup>

Toll-like receptors (TLRs), TLR2 and TLR4 in particular, are major DAMP receptors.<sup>7, 8</sup> They are expressed in various cell types, including peritoneal leukocytes and mesothelial cells.<sup>3, 9</sup> They recognise and respond to a wide range of DAMPs released following cellular stress (e.g., High

Mobility Group Box-1 [HMGB-1]; heat shock proteins [Hsp]) or generated as a consequence of matrix degradation during tissue injury (e.g., low and medium molecular mass hyaluronan [HA], fibronectin).<sup>7, 10, 11</sup> TLR triggering leads to the release of inflammatory and fibrotic mediators (e.g., IL-6, TGF- $\beta$ , TNF- $\alpha$ , IL-8).<sup>2, 8</sup>

Given the damaging pro-inflammatory and pro-fibrotic effects that may result from a prolonged exposure to PDS (conventional or more bio-compatible) and the major role that TLRs play in DAMPs-induced pro-inflammatory and pro-fibrotic responses, we conducted *in vitro*, *ex vivo* and *in vivo* studies to: 1) evaluate the capacity of different PDS to elicit pro-inflammatory and fibrotic responses and induce DAMP generation by peritoneal cells; 2) identify the main PDS-induced pro-inflammatory DAMPs; 3) assess the involvement of peritoneal TLR2 and TLR4 in PDS-induced DAMPs-mediated pro-fibrotic responses and 4) evaluate a TLR-based potential therapeutic strategy to prevent PDS-induced peritoneal fibrosis. The study reveals a major role of TLR2 and TLR4 in PDS-associated sterile peritoneal inflammation and fibrosis development, identifies Hsp70 and HA as main TLR activating pro-inflammatory DAMPs induced by peritoneal exposure to PDS and demonstrates the therapeutic potential of blunting peritoneal TLR activity to prevent PDS-induced fibrosis by using a TLR modulator, the soluble form of TLR2.

## RESULTS

### **Pro-inflammatory and pro-fibrotic effects of different PD solutions on primary human peritoneal leukocytes and mesothelial cells**

We first evaluated the capacity of a range of PDS to elicit pro-inflammatory and pro-fibrotic responses from the main peritoneal cell types involved in the initial response to danger: leukocytes and mesothelial cells (Figure 1, a and b). Widely used PDS either glucose-based (1.36% and 2.27% glucose Dianeal®, Physioneal®, Stay Safe®) or icodextrin-based (Extraneal®) (Supplementary Table S1), having low pH (Dianeal®, Extraneal®, Stay Safe®) or physiologic pH (Physioneal®), were tested. All PDS tested induced, to a varying extent, the release of inflammatory and fibrotic mediators by non-infected peritoneal dialysis effluent-isolated uremic leukocytes (Figure 1a) and mesothelial cells (HPMC, from greater omentum; Figure 1b). Physioneal® was the least stimulatory PDS tested, as it did not induce the release of any of the pro-fibrotic and/or pro-inflammatory cytokines tested: CXCL-8/IL-8, IL-6, TNF- $\alpha$ , TGF- $\beta$  and IL-1 $\beta$  – the latter a prototypical inflammasome-derived cytokine – by HPMC, and it induced very low levels, or did not induce, CXCL-8/IL-8 and IL-1 $\beta$  by peritoneal leukocytes from half the patients tested. The low response of HPMC to Physioneal® was maintained even after 24h exposure to uremic medium (Supplementary Figure S1). The results shown here are of one patient representative of all patients for each cytokine tested. The data in Supplementary Figure S2 demonstrates that the results are truly representative by using as an example the PDS induced IL-8 in leukocytes and HPMC for each patient (leukocytes, n=8; HPMC, n=6) as well as the combined data. Of note, as a result of inter-patient variability, the combined data for HPMC (Supplementary Figure S2 b, inset) did not show statistical significance, although the results obtained for each individual donor were significant.

To further evaluate the effect of PDS on peritoneal cells, we focused on the effect of low-glucose Dianeal® (1.36% glucose, Dianeal/low), the most commonly used PDS in our Nephrology Unit, and used it as experimental model. We analyzed inflammatory and immunity-related gene

expression in uremic peritoneal leukocytes and HPMC exposed to Dianeal/low for 16h (Figure 1, c and d and Table 1 and 2; full list of genes tested in Supplementary Table S2 and S3). Fifteen genes were found significantly induced ( $P < 0.05$ ; fold change  $\geq 2$ ) in leukocytes by Dianeal/low at this time point and only 5 were down-modulated ( $P < 0.05$ ; fold change  $\leq 0.5$ ). Notably, among the transcripts induced by the PDS were those coding for inflammatory mediators (CXCL8/IL-8, TNF- $\alpha$ , IFN- $\gamma$ , monocyte chemoattractant CCL2/MCP-1, the chemokine receptor CCR4, IL-1 $\beta$ ) as well as for TLR2, its two signaling partners (TLR1 and TLR6), TLR3, and TLR signal intermediates (MAPK, TRAF-6, TICAM1). HPMC exposure to Dianeal/low resulted in 8 genes being significantly induced and 6 down-modulated (Figure 1d; Table 2). Among the affected transcripts, those for the pro-inflammatory cytokines IL- $\alpha$ , IL- $\beta$  and CXCL8/IL-8 were found strongly up-modulated, whereas that for the anti-inflammatory cytokine CXCL10/IL-10 was down-modulated. Additional fibrosis gene expression analysis in Dianeal/low-exposed HPMC – the cell type known to contribute to peritoneal fibrosis by acquiring a fibroblastic phenotype following epithelial-to-mesenchymal transdifferentiation (EMT) – showed a 3-fold increase in the expression of *VGEFA* (main isoform of VEGF) and a reduction in *E-cadherin* (Supplementary Figure S3), both effects indicating EMT.<sup>12, 13</sup>

### **Involvement of TLR2 and TLR4 in PD solution-induced peritoneal production of inflammatory and fibrotic mediators**

To test whether TLR2 and/or TLR4 – main TLRs involved in sterile inflammatory responses – were involved in the inflammatory and fibrotic responses of peritoneal cells exposed to PDS, TLR2 and TLR4 blocking experiments were conducted (Figure 2, a-c). mAb blocking of peritoneal leukocyte TLR2 or TLR4 inhibited Dianeal/low-induced pro-inflammatory cytokine release (IL-8), and the extent of the inhibition depended on the PD patient tested (Figure 2a). Simultaneous TLR2 and TLR4 blockade resulted in a stronger inhibition. These findings indicated that TLR2 and TLR4 ligand(s) and/or ligands capable of being recognized by both TLR2 and TLR4 were involved. A significant reduction in the release of IL-8 was also observed when TLR2 was blocked in PDS-

exposed HPMC (Figure 2b). Of note, mAb blocking of TLR4 was not tested in HPMC, as they do not express TLR4<sup>3, 9</sup>, and did not respond to LPS (TLR4 ligand) even after 24h exposure to uremic medium (Supplementary Figure S1).

Analysis of the release of a range of pro-inflammatory and fibrotic cytokines by uremic peritoneal leukocytes exposed to PDS following TLR2+TLR4 blockade was also conducted (Figure 2c). The release of most of the cytokines induced by Dianeal/low was significantly inhibited, to a varying extent, by TLR2/4 blocking. Collectively, these findings indicated that peritoneal TLR2 and TLR4 drive inflammatory and fibrotic responses to existing components of the PDS and/or to endogenous DAMPs that may be generated/released as a consequence of cellular stress resulting from exposure to PDS.

To investigate whether the PDS contains components capable of direct TLR activation, the rapid phosphorylation of extracellular signal-regulated protein kinase 1/2 (ERK1/2) – a typical TLR signal intermediate<sup>14</sup> – was evaluated following a short exposure to Dianeal/low (Figure 3a). Peritoneal leukocyte exposure to PDS for up to 60 min did not induce ERK1/2 phosphorylation. By contrast, leukocyte exposure to sterile (non-infected) PD effluent collected from PD patients induced rapid ERK1/2 phosphorylation, suggesting the presence of TLR DAMPs in the effluent. As expected, short exposure to the TLR agonists Pam<sub>3</sub>-Cys-Ser-(Lys)<sub>4</sub> (Pam<sub>3</sub>Cys; a synthetic bacterial lipopeptide and TLR2 agonist) and lipopolysaccharide (LPS, endotoxin, a TLR4 agonist) resulted in strong ERK1/2 phosphorylation (Figure 3a). Control experiments (Figure 3b) confirmed that TLR activation induced ERK phosphorylation, as TLR2- and/or TLR4-specific mAb blocked Pam<sub>3</sub>Cys- (anti TLR2), LPS- (anti TLR4) and PD effluent- (anti TLR2 and anti TLR4) induced phosphorylation. We also tested the rapid degradation upon TLR activation of the nuclear factor kappa-B (NF-κB) inhibitory protein IκB-α, which inhibits the nuclear translocation of NF-κB and thus its transcription activator activity.<sup>15</sup> Pam<sub>3</sub>Cys induced a rapid and progressive reduction over 30 min in the expression of IκB-α in peritoneal leukocytes (Figure 3c), and by 60 min the level of IκB-α was recovering. By contrast, leukocyte exposure to Dianeal/low did not show variations over



time in I $\kappa$ B- $\alpha$  expression. Together, these findings indicated that peritoneal exposure to PDS leads to TLR2 and TLR4 activation by inducing DAMP generation, as the PDS does not appear to contain pre-existing components capable of direct TLR activation.

### **Identification of Hsp70 and HA as main pro-inflammatory TLR activating DAMPs induced by peritoneal cell exposure to PD solutions**

To identify the main DAMPs generated by peritoneal cell exposure to PDS, the presence of a panel of well-described DAMPs, including endogenous proteins (Hsp60, Hsp70, HMGB-1, calprotectin), and extracellular matrix proteoglycans and glycosaminoglycans (decorin, fibronectin, versican, biglycan and HA) was first tested in non-infected PD effluent from PD patients (Figure 4a). Consistent with the rapid triggering of ERK1/2 phosphorylation, most DAMPs tested were present in PD effluents, to a varying extent depending on the patient, except for versican and biglycan which were not detected. To identify the DAMPs preferentially induced by exposure to PDS, uremic peritoneal leukocytes and HPMC were incubated overnight with Dianeal/low (Figure 4, b and c). Leukocytes (Figure 4b) showed constitutive release of the DAMPs tested, except for biglycan, which was not detected either before or upon exposure to Dianeal/low. Notably, exposure to PDS increased the release of only two DAMPs, Hsp60 and Hsp70, both known TLR2 and TLR4 ligands<sup>7</sup>, whereas the others were either not affected (HMGB-1, fibronectin) or inhibited (decorin, calprotectin, HA, versican). HPMC also showed constitutive release of DAMPs, except for versican and biglycan, which were not detected either before or following exposure to the PDS (Figure 4c). In this case, PDS increased the release of Hsp60, Hsp70 and also HA, the latter also a TLR2 and TLR4 ligand,<sup>7, 11</sup> whereas the remaining DAMPs were not significantly affected. This pattern of DAMP expression was also observed when peritoneal cells were exposed to Dianeal/high®, Physioneal®, Stay Safe® or Extraneal® (Supplementary Figure S4). Of note, the detected DAMPS may result from *de novo* synthesis and/or active or passive release – the latter as a consequence of cellular damage – induced by the PDS.

We next tested whether the DAMPs released by peritoneal cells upon exposure to PDS were capable of inducing cell activation via TLRs (Figure 5a). Purified Hsp70 as well as low (~33 kDa) and medium (~289 kDa) molecular mass HA, but not Hsp60, induced a rapid increase in the percentage of uremic peritoneal macrophages expressing phosphorylated ERK1/2, increasing from 15 min to 60 min (Figure 5a). A similar ERK1/2 phosphorylation profile was observed when non-infected PD effluent from PD patients was tested, whereas the TLR2 agonist Pam<sub>3</sub>Cys induced an even stronger phosphorylation pattern (Figure 5a). Of note, Hsp70 and HA – identified here as capable of inducing ERK phosphorylation – are each recognised by both TLR2 and TLR4. These findings were consistent with those shown in Figure 2, demonstrating that the pro-inflammatory/fibrotic effects exerted by PDS on peritoneal cells can be inhibited by TLR2/4 blockade. Together, these findings indicated that peritoneal cell exposure to PDS increases the release of three DAMPs: Hsp60, Hsp70 and HA, and that, by a TLR2/TLR4-mediated pathway, Hsp70 and HA but not Hsp60, are capable of eliciting inflammatory responses from peritoneal cells. Consistent with this conclusion, pharmacologic inhibition of Hsp70 or HA blockade by an HA-specific inhibitory peptide<sup>16</sup> significantly inhibited peritoneal cell inflammatory responses to PDS (Figure 5b). These findings supported the potential of controlling DAMP-TLR interactions as a therapeutic strategy against peritoneal fibrosis.

### **Capacity of the TLR inhibitor soluble TLR2 to modulate PDS-induced peritoneal leukocyte inflammatory and fibrotic responses *in vitro***

The therapeutic potential of reducing peritoneal TLR activity by inhibiting DAMP-TLR interactions was next evaluated *in vitro*. We tested the inflammation regulatory capacity of the inhibitor of TLRs, soluble Toll-like receptor 2 (sTLR2), which we previously demonstrated to reduce infection-induced TLR-mediated peritoneal inflammation and fibrosis by binding to TLR2 ligands and acting as a decoy receptor.<sup>3, 17-19</sup> Given that the PDS-induced TLR activating DAMPs Hsp70 and HA are recognised by both TLR2 and TLR4, sTLR2 would be able to interfere with both TLR2 and TLR4 triggering by interacting with these DAMPs. Figure 6 shows that most pro-inflammatory and

fibrotic cytokines released by PDS-exposed peritoneal uremic leukocytes were inhibited by sTLR2. These findings demonstrated that sTLR2 is a potent inhibitor of PDS-associated sterile inflammation, and may be of therapeutic value against subsequent fibrosis development in PD.

### **Prevention of PDS-induced peritoneal fibrosis development *in vivo* by therapeutic administration of sTLR2**

To evaluate the therapeutic potential of sTLR2 against peritoneal inflammation and fibrosis resulting from prolonged exposure to PD solutions *in vivo*, a validated mouse model of sterile peritoneal fibrosis was used.<sup>20</sup> In this model, the morphological and functional alterations of the peritoneal membrane observed in non-infected patients on PD are mimicked by twice daily peritoneal infusion (40 days) through a catheter of a standard PDS (Figure 7a and Refs<sup>20, 21</sup>). Similar to human uremic peritoneal cell exposure to PDS (Figure 4), in this model the daily infusion of PDS resulted in increased peritoneal release of Hsp60, Hsp70 and HA (Figure 7b). Furthermore, mouse peritoneal TLR2/4, like the humans' (Figure 2), appear as major receptors recognising DAMPs induced by PDS, as exposure of TLR2 or TLR4 deficient mice-derived peritoneal leukocytes to PDS resulted in a marked reduction in pro-inflammatory and fibrotic cytokine induction when compared to leukocytes from wild type mice (Figure 7c).

Daily infusion of PDS led to robust peritoneal fibrosis by day 40, as judged by the thickening of the sub-mesothelial compact zone observed in parietal membrane sections (Figure 8a). This was accompanied by a not statistically significant trend to increase in the peritoneal levels of the inflammatory mediators TNF- $\alpha$ , IL-1 $\beta$ , KC (murine functional counterpart of human IL-8, a PMN chemoattractant), IL-6 (also a major driver of peritoneal fibrosis<sup>2</sup>), and the pro-inflammatory and fibrotic cytokine IFN- $\gamma$ . No effect on MCP-1 (a monocyte chemoattractant) was observed (Figure 8b). The increase in inflammatory mediators resulted in an overall increase in peritoneal leukocyte numbers and percentage of recruited neutrophils in particular (Figure 8c). The unchanged percentage of monocytes – although the absolute number may be increased, as the total leukocyte number is increased – in the face of the increase in neutrophils in response to PDS may contribute

to the chronicity of the inflammatory process which leads to fibrosis by delaying normal resolution of inflammation. Fibrosis development was also accompanied by a slight reduction in regulatory T cells (Treg). This anti-inflammatory T cell subset controls T cell expansion, including of inflammatory Th17 cells, which are known to be involved in peritoneal damage and fibrosis development<sup>22</sup>. The percentage of Th17 cells, however, was not affected (Figure 8c). Consequently, the ratio Treg:Th17 in the PDS-instilled mice was reduced (Figure 8c).

Co-administration of sTLR2 twice weekly with the PDS prevented peritoneal fibrosis development (Figure 8a). Consistent with this finding, sTLR2 suppressed the PDS-induced increase of all inflammatory and fibrotic mediators tested (Figure 8b), resulting in very low levels of cytokines, similar to those induced by the catheter infusion of PBS. sTLR2's suppressive effect on inflammatory mediators was followed by a marked reduction in peritoneal leukocyte numbers and percentage of infiltrating neutrophils in particular, but no effect on monocytes (Figure 8c). Notably, sTLR2 administration recovered Treg cells to levels similar to those observed by PBS infusion, increasing albeit not significantly the Treg:Th17 ratio (Figure 8c).

Analysis of fibrosis-related gene transcripts in mice peritoneal membranes conducted after the last PDS+sTLR2 infusion (day 40) (Figure 8d, Table 3) showed a marked inhibitory effect of sTLR2 on the capacity of PDS to induce mRNA coding for a number of inflammatory mediators and fibrosis markers (full list of genes in Supplementary Table S4). Twenty-nine of the 85 genes tested were significantly induced ( $P < 0.05$ ; fold change  $\geq 2$ ) by PDS at this time point, and sTLR2 reduced this effect in 27 of them. Among the transcripts inhibited by sTLR2 was *FasI*, which was strongly induced by PDS. FasL is central to apoptosis, a cell death mechanism that impairs bacterial clearance during PD, induces peritoneal macrophage death, and increases peritoneal inflammation and the production of PMN chemoattractants.<sup>23, 24</sup> sTLR2 administration also inhibited the PDS-induced transcription of signal transducer and activator of transcription 1 (STAT-1) (Table 3), a critical signal intermediate for fibrosis development.<sup>2</sup> Together with STAT-1, IFN- $\gamma$  has been demonstrated to mediate peritoneal fibrosis,<sup>2</sup> and sTLR2 significantly reduced the strong PDS-

induced transcription of IFN- $\gamma$  (Table 3). A number of transcripts for matrix metalloproteinases (MMPs), which are involved in both augmenting and attenuating fibrosis,<sup>25</sup> were induced by PDS and reduced by sTLR2, likewise a number of the negative regulators of MMPs, tissue inhibitor of metalloproteinases-1 to 3 (TIMP-1/3). Similarly, the PDS-induced transcription of the pro-fibrotic cytokine TGF- $\beta$  and its receptor TGF- $\beta$ R2, and that of the inflammatory mediators IL-1 $\beta$  and TNF- $\alpha$  were strongly reduced by sTLR2 administration. Thus, the therapeutic administration of sTLR2 can prevent peritoneal fibrosis development induced by prolonged exposure to PD fluids by acting on a number of pro-inflammatory and fibrotic mediators and controlling inflammatory cell expansion.

## DISCUSSION

The long-term PD-associated progressive peritoneal membrane injury resulting in sterile peritoneal inflammation and fibrosis has been well documented.<sup>5, 6</sup> The prolonged exposure to conventional PDS has been demonstrated to substantially contribute to peritoneal membrane injury and chronic low-grade inflammation<sup>26</sup> and a number of biomarkers have been evaluated in an attempt to help improve PD patient outcomes.<sup>27</sup> Acidic pH, high glucose concentrations and high levels of glucose degradation products in PDS have all been reported to cause local inflammation with resultant adverse functional outcomes, such as higher peritoneal solute transport rate (PSTR) and membrane failure due to fibrosis. Therefore, more bio-compatible PDS were developed aimed at mitigating some of these adverse effects. They include, neutral pH, low or ultralow glucose degradation products containing solutions, solutions using alternative osmotic agents, low-sodium solutions and supplementation with the dipeptide alanyl-glutamine.<sup>28-31</sup> The peritoneal administration of alanyl-glutamine - a dipeptide with immunomodulatory effects - in uremic rat and mouse PD exposure models showed substantial promise, as it reduced PD-induced peritoneal fibrosis, reduced pro-inflammatory/fibrotic markers and ameliorated damage, in part by modulating IL-17 expression.<sup>31</sup> At present, however, in spite of demonstrating some beneficial effects in maintaining stability of PSTR, there is no conclusive clinical evidence that the use of more bio-compatible PDS is associated with a lower burden of peritoneal inflammation or improved clinical outcomes.<sup>32</sup> Notably, data from the GLOBAL Fluid study have shown that the peritoneal levels of the pro-inflammatory and fibrotic cytokine IL-6 are strongly associated with patients PSTR,<sup>33</sup> confirming a link between local inflammation and membrane function. A number of intervention studies have not yet been able to define effective strategies to consistently lower the inflammatory burden in long-term PD patients.<sup>1</sup> This has highlighted the importance of defining the underlying processes that drive the chronic inflammatory state that develops upon prolonged exposure to PDS. Critically, studies to identify the main peritoneal receptors involved in triggering the initial pro-inflammatory/fibrotic responses to PDS, and develop therapeutic strategies to reduce their

activation have not been conducted. In the present study, we identified Hsp70 and HA as main pro-inflammatory and fibrotic DAMPs induced by exposure to PDS, and their receptors, TLR2 and TLR4, as major therapeutic targets against PDS-induced fibrosis development. We described a therapeutic strategy to prevent PDS-induced fibrosis that targets TLRs and DAMP-TLR interactions by using a decoy soluble receptor, sTLR2.

The potential therapeutic benefit of targeting TLRs and their interaction with DAMPs upon peritoneal exposure to PDS was demonstrated by the pivotal role that TLR2 and TLR4 showed in mediating pro-inflammatory and fibrotic responses to Hsp70 and HA and to Dieneal *ex vivo* in patients' uremic peritoneal leukocytes, and the conclusive demonstration that disrupting peritoneal TLR triggering *in vivo* with sTLR2 fully prevented PDS-induced fibrosis development. The protective effect of sTLR2 *in vivo* may result at least in part from neutralising the TLR2/4 activating DAMPs Hsp70 and HA that were found increased following daily peritoneal infusion of PDS. However, the involvement in mice of additional TLR2/4 DAMP ligands, also targeted by sTLR2, cannot be excluded. It has been reported that PDS-induced intracellular upregulation of Hsp may be anti-inflammatory by conferring cytoprotection, mediating cellular repair and improving the integrity of the cellular membrane, thus reducing pro-inflammatory DAMP leakage from stressed cells.<sup>34-36</sup> It is not clear whether in the present study Hsp70 is being upregulated by PDS exposure, however, its increased release following PDS exposure may be associated with loss of cell membrane integrity and of Hsp cytoprotective effect. The mechanism underlying sTLR2's anti-fibrotic effect appears to be related to maintaining low levels of infiltrating leukocytes, rescuing Treg cell levels, as well as maintaining very low peritoneal levels of inflammatory mediators. This latter effect was not statistically significant when compared with that of PDS infusion alone, except for that on IL-6. However, sTLR2 administration did reduce inflammatory mediators to levels similar to those induced by the catheter infusion of PBS, which had no significant impact on fibrosis. The non-statistical significance of the sTLR2 effect on inflammatory mediators is most likely due to the fact that the exposure to PDS alone resulted in a non-statistically significant

increase in inflammatory mediators. This low-grade, chronic inflammation, when maintained over a long period of time (e.g., 40 days in this model) is sufficient to induce fibrosis, as demonstrated here and as has been previously documented.<sup>37</sup> Thus, in the presence of sTLR2, the PDS-driven inflammatory response appears to be maintained very low, below the threshold for fibrogenesis. This supports our previous finding that the intensity of local inflammation is directly related to fibrosis development.<sup>3</sup> Thus, controlling the intensity of the TLR-mediated inflammation with sTLR2 appears as an efficient therapeutic strategy against PDS-induced peritoneal fibrosis. The efficacy of sTLR2 to reverse ongoing fibrosis, as opposed to prevent it, however remains to be assessed.

To date, a main target for therapeutic intervention has been the pro-fibrotic cytokine TGF- $\beta$ . Inhibition of its synthesis (e.g., angiotensin-converting enzyme inhibitors [enalapril]; angiotensin receptor blockers [losartan]) or activity (e.g., anti TGF- $\beta$  peptide; gene transfer of decorin – a TGF- $\beta$  inhibiting proteoglycan) showed promising effects *in vitro* and in some preclinical studies.<sup>5, 21, 38-42</sup> However, blocking TGF- $\beta$  is potentially hazardous given its pleiotropic functions, including in normal embryonic development, tumorigenesis and tumour progression, as well as its pro- and anti-inflammatory activity.<sup>43, 44</sup> Furthermore, TGF- $\beta$  is just one of many fibrosis mediators acting downstream of TLR activation. sTLR2 presents a clear advantage over these strategies, as it is capable of modulating the production of a range of inflammatory and fibrosis mediators by controlling the initial triggering of TLR2 and TLR4 by their common DAMP ligands. The efficacy of this strategy may extend to the control of inflammation/fibrosis resulting from TLR2/4 DAMP ligands released as a consequence of the uremic milieu and/or the peritoneal catheter.

We have previously demonstrated the capacity of sTLR2 to inhibit peritoneal infection-induced fibrosis without compromising bacterial clearance.<sup>3</sup> This feature of sTLR2 would present an advantage over therapies based on a complete TLR blockade to achieve anti-inflammatory effects e.g., by combining anti-TLR2 and -TLR4 antibodies,<sup>45</sup> considering that sTLR2 would be used in patients on PD, who are prone to infections. The sTLR2-based anti-fibrotic strategy



described here could thus prove to be a valuable adjunct to more bio-compatible PD solutions. Furthermore, the potential benefit of sTLR2 in other PD-associated inflammatory conditions deserves to be evaluated, for example, to help reduce the elevated risk of cardiovascular diseases or the occurrence of encapsulating peritoneal sclerosis; in kidney fibrosis, as well as to reduce sterile inflammation associated with acute kidney injury.

## MATERIALS AND METHODS

### Cells and PD effluent

Samples from healthy individuals (omentum) and PD patients (spent PD effluent) were obtained in accordance with the institutional review board of Cardiff University and the local National Health Service Research Ethics Committee. Written informed consent was obtained from all donors. Sampling was carried out within the UK Clinical Research Network under study portfolios ID #11838 (PERITPD) and ID #11839 (LEUKPD) and adhered to the Declaration of Helsinki. Spent PD effluents were obtained from continuous ambulatory PD patients following an overnight dwell. The sterility of the effluents used was confirmed by bacterial DNA testing by qPCR as previously described.<sup>3</sup> Peritoneal leukocytes were obtained from non-infected PD effluents (PDE) by centrifugation as previously described<sup>3</sup>. Peritoneal lymphocytes were differentiated from monocytes/macrophages and neutrophils using flow cytometry on the basis of their forward and side scatter properties and CD14 staining (lymphocytes: CD14<sup>-</sup>; monocytes/macrophages: CD14<sup>+high</sup>; neutrophils: CD14<sup>+low</sup>). Monocytes/macrophages were the predominant cell population in PDE derived from non-infected (stable) patients, consistently accounting for 60-80% of leukocytes, which was in agreement with previous reports<sup>3,46</sup>, whereas the number of neutrophils was negligible. The main non-infected PDE-derived peritoneal cell type responding to TLR ligands were the monocytes/macrophages, not the lymphocytes, as we previously demonstrated.<sup>3</sup> Additional CD45 staining was used to differentiate mesothelial cells (CD45<sup>-</sup>) from leukocytes (CD45<sup>+</sup>). Typically, mesothelial cells accounted for  $\leq 5\%$  of the PDE cell population (Supplementary Figure S5). Leukocytes were cultured in RPMI 1640 medium (Invitrogen, Carlsbad, CA) supplemented with 1% foetal calf serum (FCS, HyClone Laboratories, Logan, UT;  $< 0.06$  U/mL endotoxin). All experiments were conducted with cells isolated from a single dwell/dialysate (not pooling) from each patient. The cell-free (centrifuged) PD effluents were aliquoted and kept frozen ( $-85^{\circ}\text{C}$ ) until further use. All effluents used were from uremic patients (urea  $> 7.8$  mM; creatinine  $> 110$   $\mu\text{M}$ ; U.K.-wide criteria defined by the National Health Service). Of note, the expression of TLR2/4 in

uremic macrophages was not affected after a 16h culture in a non-uremic milieu (Supplementary Figure S6). HPMC were prepared by tryptic digest of omental biopsies of non-PD patients, as previously described<sup>9</sup> and cultured in M199 medium (Invitrogen) supplemented with insulin (0.5 µg/ml), transferrin (0.5 µg/ml), and 10% FCS. The viability of peritoneal leukocytes and mesothelial cells was routinely tested following their overnight (16h) exposure to PD solutions. Macrophage and lymphocyte viability was always 85-95% and mesothelial cells 70-90%, depending on the PDS solution (Supplementary Figure S7).

Murine peritoneal leukocytes (Fig. 7c) were obtained by peritoneal lavage (2ml PBS) of 8 to 10-wk-old C57BL/6 wild-type, TLR2<sup>-/-</sup> and TLR4<sup>-/-</sup> female mice (Charles River Laboratories, Wilmington, MS)

### **Functional assays**

For activation experiments, triplicate aliquots of primary human/mouse peritoneal leukocytes ( $2.5 \times 10^4$  cells/well, in 96-well plates), or HPMC ( $4 \times 10^4$  cells/well, in 48 well-plates), were cultured in the presence of the indicated PDS (1:2 dilution). For blocking experiments, cells were preincubated (30 min at 37°C) with functional grade anti-TLR2 (clone T2.5, Hycult Biotech, Uden, Netherlands), anti-TLR4 (clone 3C3, Hycult), their corresponding isotype-matched control (5 µg/ml), the Hsp70 inhibitor VER155008 (20µM, Tocris, Bio-Techne Ltd, Abingdon, U.K.), the HA inhibitory peptide Pep-1, the scrambled peptide control (250 µg/ml, Genscript, Oxon, U.K.), or human recombinant sTLR2 (250 ng/ml, low endotoxin, R&D Systems, Minneapolis, MN) before addition of PDS or the synthetic bacterial lipopeptide Pam<sub>3</sub>-Cys-Ser-(Lys)<sub>4</sub> HCl (250 ng/ml, EMC microcollections, Tübingen, Germany).

Culture supernatants were collected after 16h and cytokines and DAMPs quantified by single (R&D) or multiplex ELISA (Meso Scale Discovery, Rockville, MD). For TGF-β determinations, cells were washed after 48h stimulation and cultured for a further 24h in FCS-free medium before culture supernatant collection and ELISA. Following cell stimulations, cell viability was assessed

by flow cytometry using the eFluor viability dye (eBioscience, San Diego, CA) and was always  $\geq 75\%$  and unaffected by exposure to PDS.

To evaluate ERK1/2 phosphorylation and I $\kappa$ B- $\alpha$  degradation, cells ( $5 \times 10^5$ /condition) were stimulated or not with Dianeal/low (1:2 dilution), sterile PD effluent (1:2 dilution), Pam<sub>3</sub>Cys (250 ng/ml), LPS (50 ng/ml, Invivogen, San Diego, CA), recombinant Hsp70 (500 ng/ml, Abcam, Cambridge, U.K.), recombinant Hsp60 (500 ng/ml, Enzo Life Sciences, Exeter, U.K.) and low (~33 kDa) or medium (~289 kDa) molecular mass hyaluronan (both at 100  $\mu$ g/ml, R&D) following preincubation or not with anti-TLR2 or anti-TLR4 blocking mAbs or an isotype control. At the indicated time points, activation was stopped by addition of paraformaldehyde (5% final concentration, ERK1/2) or lysis buffer (I $\kappa$ B- $\alpha$ ).

### **Flow cytometry**

ERK1/2 phosphorylation was evaluated by flow cytometry<sup>47</sup> following cell fixation using an Alexa-Fluor 647-conjugated ERK1/2 phosphorylated-specific mAb according to the manufacturer's instructions (BioLegend).

### **Western blotting**

I $\kappa$ B- $\alpha$  degradation was tested by Western Blot as previously described<sup>47</sup>. Cell lysates were diluted 1:2 in Laemmli reducing sample buffer and subjected to 10% SDS-PAGE prior to Western blot analysis using an anti-I $\kappa$ B- $\alpha$  antibody (clone #417208, R&D) or an anti- $\alpha$ -tubulin antibody (clone #961216, R&D) as a loading control. Densitometric analysis was performed using the ImageJ software.

### **Gene arrays**

Total RNA was isolated from peritoneal leukocytes, HPMC or mice peritoneal membranes using the RNeasy mini kit (Qiagen, Germantwon, MD). RT was performed on 200 ng RNA using the RT<sup>2</sup> first strand kit (Qiagen, including a genomic DNA elimination step). qPCR was performed on the resulting cDNA using the human Innate and Adaptive Immune Response or the mouse Fibrosis RT<sup>2</sup>

Profiler PCR Array (84 genes; Qiagen) and the ABI QuantStudio 12K Flex PCR System (Thermo Fisher Scientific, U.K.). The results were analysed using Qiagen software. Changes in gene expression compared to control were considered statistically significant when  $P < 0.05$ , and biologically relevant when the fold change was  $\leq 0.5$  or  $\geq 2$ , as recommended by the manufacturer. The complete data sets are shown in Supplementary Table S2, S3 and S4.

### ***In Vivo* experiments**

All procedures were carried out under a project license granted by the Spanish Consejo Superior de Investigaciones Científicas. Inbred 8 to 10-wk-old wild-type female mice (C57/BL6J) underwent peritoneal catheter (Access technologies, West Midlands, U.K.) implantation surgery, as previously reported<sup>20</sup> (Supplementary Figure S8). Following recovery (7 days), mice were instilled twice daily for 40 days with 2 ml Fresenius Standard 4.25% glucose solution (n=8) or PBS (n=5) in the absence or presence of recombinant sTLR2 (100 ng/ml, added three times per week). After 40 days, mice were sacrificed, peritoneal lavages were obtained (2ml PBS), and two sets of parietal peritoneal membrane biopsies were taken. One set was used for membrane histology (below) and the second set was snap-frozen in liquid nitrogen for RNA extraction and gene expression studies (above). Leukocyte numbers in the lavages were determined by automated counting (Scepter automated cell counter, Merk Millipore, Leicester, U.K.), and cell populations were identified by differential staining (anti-CD11b, anti-Gr1, anti-F4/80, anti-CD3, anti-CD4, anti-CD8, anti-Foxp3, anti-IL-17, BD biosciences, Oxford, U.K.) and flow cytometric analysis. Cytokine levels were determined by multiplex ELISA.

### **Peritoneal membrane histology**

Parietal peritoneal membrane biopsies obtained from the opposite side of the catheter were processed as previously described<sup>22</sup>. Briefly, membranes were fixed (Bouin solution), embedded in paraffin, cut into 5- $\mu$ m sections, and stained (Masson's Trichrome stain). The thickness of the SMC was determined using a Leica CTR6000 microscope and Leica Microsystems software (Milton

Keynes, U.K.). Pictures were obtained from one extreme of the biopsy to the other, and measurements taken every 50  $\mu\text{m}$ . The mean of all measurements taken from one biopsy was used as the SMC thickness for each animal.

### **Statistical analysis**

Statistical analysis of the data was performed by using an unpaired Student's *t* test. *P* values <0.05 were considered significant.

### **DISCLOSURES**

The authors declare that they have no competing interests.

## ACKNOWLEDGEMENTS

We thank Professor A. O. Phillips (Department of Nephrology, University Hospital of Wales and Cardiff University, UK), and Dr. J. E. Rey Nores (Cardiff Metropolitan University, UK) for critical comments and reading of the manuscript.

## AUTHOR CONTRIBUTIONS

A.-C.R. performed the experiments and contributed to the experimental design and writing of the manuscript. G.L.M. performed *in vivo* experiments, helped to develop the murine model of fibrosis and critically revised the manuscript. A.W. coordinated the collection and provision of tissue samples and revised the manuscript. N.T. facilitated access to patient samples and critically revised the manuscript. D.F. coordinated and facilitated access to patient samples and clinical database, and critically revised the manuscript. M.L.C. designed the *in vivo* model of fibrosis, gave input to the experimental design and critically revised the manuscript. M.O.L. designed most of the research project, provided oversight of experiments, and wrote most of the manuscript.

## SUPPLEMENTARY MATERIAL

**Figure S1.** Uremia does not affect the response to TLR2/TLR4 ligands or Physioneal® by mesothelial cells. Human peritoneal mesothelial cells (from omentum) were exposed (Uremia) or not (No uremia) to uremic PD effluent for 24h. Subsequently, cultures were washed and immediately stimulated (16h) with a TLR4 ligand (LPS, indicated concentrations), a TLR2 ligand (Pam3Cys, 100 ng/ml) or Physioneal® (1:2). The histogram plot shows the mean ( $\pm$ SD) IL-8 release after the corresponding background subtraction (exposure or not to PDE) from 1 experiment representative of 3 conducted with mesothelial cells from different donors.

**Figure S2.** PD solutions (PDS) induce pro-inflammatory responses in human peritoneal cells. Levels of IL-8 in the culture supernatants of (a) non-infected PD effluent-isolated uremic leukocytes and (b) peritoneal mesothelial cells (from omentum) following exposure (16h) to the

indicated PDS (1:2 dilution). Each plot shows the results from one donor run in triplicates ( $\pm$ SD) and the framed insets show the average of all donors tested ( $\pm$ SEM). \* $P$ <0.05; \*\* $P$ <0.01; \*\*\* $P$ <0.005 (PDS vs control).

**Figure S3.** Exposure of human peritoneal mesothelial cells to PDS induces EMT-associated gene expression changes. Gene expression levels of *Vegfa* and *E-Cadherin* in mesothelial cells (from omentum) were determined by RT-qPCR after 16h culture in the presence or absence of Dianeal/low (1:2 dilution). Histogram plots show the fold change in expression compared to the No PDS control. \*\*\* $P$ <0.005 (Dianeal/low vs No PDS). Results are of one experiment representative of three.

**Figure S4.** Human peritoneal cell exposure to PDS modulates the release of TLR DAMP ligands. Levels of TLR DAMP ligands in culture supernatants from (a) non-infected PD effluent-isolated uremic leukocytes and (b) human peritoneal mesothelial cells (from omentum) stimulated (16h) or not with the indicated PDS (1:2 dilution). Results are from one experiment ( $\pm$ SD) representative of 8 (a) and 6 (b). \*\*,  $P$ <0.01; \*\*\*,  $P$ <0.005 (PDS vs No PDS).

**Figure S5.** Cellular composition of non-infected PD effluent. Peritoneal cells were obtained by centrifugation of non-infected PD effluent and stained with CD14- and CD45-specific mAbs prior to flow cytometric analysis. Cell populations were identified on the basis of their forward and side scatter profiles and CD14 and CD45 staining. Mesothelial cells, CD45<sup>-</sup>; leukocytes, CD45<sup>+</sup>; lymphocytes, CD14<sup>-</sup>; monocytes/macrophages, CD14<sup>high</sup>; neutrophils, CD14<sup>low</sup> (typically, negligible).

**Figure S6.** Overnight culture in non-uremic milieu does not affect TLR2/4 expression by uremic macrophages. Uremic peritoneal leukocytes obtained from PD effluent were incubated (16h) in non-uremic conditions (RPMI), or in uremia-maintaining conditions (RPMI + own PD effluent 1:2). Expression levels of TLR2 (left panel) and TLR4 (right panel) on peritoneal macrophages (gated on



the basis of their forward and side scatter profiles and CD14 expression) were determined by flow cytometry. Results are representative of four independent experiments.

**Figure S7.** Viability of peritoneal cells following overnight exposure to PDS. Viability of PD effluent-isolated peritoneal leukocytes and peritoneal mesothelial cells (from omentum) following exposure for 16h to the indicated PDS (1:2 dilution). Cell viability was routinely determined by flow cytometry following staining with the viability dye efluor 647.

**Figure S8.** Surgical procedure of peritoneal catheter insertion in mice. Inbred 8 to 10-wk-old wild-type female mice (C57/BL6J) underwent surgery under general anaesthesia. Animals were shaved and a large incision was made in the skin on the right flank of the mouse, followed by a small incision of the peritoneal muscle layer, through which the tip of the catheter was inserted into the peritoneal cavity (**a**). The muscle layer was sutured back, ensuring that the catheter would stay in position, and the injection port (**b**) was inserted under the skin in a dorsal position (**c**) before suturing the skin (**d**). The final position of the catheter and injection port is shown in (**e**). One week after surgery, a specially-designed blunt needle was used to pierce the skin and inject the PDS into the catheter through the injection port without damaging it.

**Table S1.** Characteristics of the peritoneal dialysis solutions used.

**Table S2.** Effect of Dianeal/low (PDS) on inflammation and immunity-related gene expression by human uremic peritoneal leukocytes (complete gene array).

**Table S3.** Effect of Dianeal/low (PDS) on inflammation and immunity-related gene expression by human peritoneal mesothelial cells (complete gene array).

**Table S4.** Effect of sTLR2 on fibrosis-related peritoneal gene expression in mice continuously exposed to PDS for 40 days (complete fibrosis gene array)

**Supplementary information is available at *Kidney International's* website**

## REFERENCES

1. Cho Y, Hawley CM, Johnson DW. Clinical causes of inflammation in peritoneal dialysis patients. *International journal of nephrology* 2014; **2014**: 909373.
2. Fielding CA, Jones GW, McLoughlin RM, *et al.* Interleukin-6 signaling drives fibrosis in unresolved inflammation. *Immunity* 2014; **40**: 40-50.
3. Raby AC, Colmont CS, Kift-Morgan A, *et al.* Toll-Like Receptors 2 and 4 Are Potential Therapeutic Targets in Peritoneal Dialysis-Associated Fibrosis. *Journal of the American Society of Nephrology : JASN* 2017; **28**: 461-478.
4. Flessner MF, Credit K, Henderson K, *et al.* Peritoneal changes after exposure to sterile solutions by catheter. *Journal of the American Society of Nephrology : JASN* 2007; **18**: 2294-2302.
5. Tomino Y. Mechanisms and interventions in peritoneal fibrosis. *Clinical and experimental nephrology* 2012; **16**: 109-114.
6. Strippoli R, Moreno-Vicente R, Battistelli C, *et al.* Molecular Mechanisms Underlying Peritoneal EMT and Fibrosis. *Stem cells international* 2016; **2016**: 3543678.
7. Anders HJ, Schaefer L. Beyond tissue injury-damage-associated molecular patterns, toll-like receptors, and inflammasomes also drive regeneration and fibrosis. *Journal of the American Society of Nephrology : JASN* 2014; **25**: 1387-1400.
8. Kawasaki T, Kawai T. Toll-like receptor signaling pathways. *Frontiers in immunology* 2014; **5**: 461.
9. Colmont CS, Raby AC, Dioszeghy V, *et al.* Human peritoneal mesothelial cells respond to bacterial ligands through a specific subset of Toll-like receptors. *Nephrology, dialysis, transplantation : official publication of the European Dialysis and Transplant Association - European Renal Association* 2011; **26**: 4079-4090.
10. Chen GY, Nunez G. Sterile inflammation: sensing and reacting to damage. *Nat Rev Immunol* 2010; **10**: 826-837.
11. Jiang D, Liang J, Fan J, *et al.* Regulation of lung injury and repair by Toll-like receptors and hyaluronan. *Nat Med* 2005; **11**: 1173-1179.
12. Yung S, Chan TM. Pathophysiological changes to the peritoneal membrane during PD-related peritonitis: the role of mesothelial cells. *Mediators of inflammation* 2012; **2012**: 484167.
13. Ruiz-Carpio V, Sandoval P, Aguilera A, *et al.* Genomic reprogramming analysis of the Mesothelial to Mesenchymal Transition identifies biomarkers in peritoneal dialysis patients. *Scientific reports* 2017; **7**: 44941.

14. Peroval MY, Boyd AC, Young JR, *et al.* A critical role for MAPK signalling pathways in the transcriptional regulation of toll like receptors. *PloS one* 2013; **8**: e51243.
15. Ghosh S, Hayden MS. New regulators of NF-kappaB in inflammation. *Nat Rev Immunol* 2008; **8**: 837-848.
16. Mummert ME, Mohamadzadeh M, Mummert DI, *et al.* Development of a peptide inhibitor of hyaluronan-mediated leukocyte trafficking. *J Exp Med* 2000; **192**: 769-779.
17. Raby AC, Le Boudier E, Colmont C, *et al.* Soluble TLR2 reduces inflammation without compromising bacterial clearance by disrupting TLR2 triggering. *J Immunol* 2009; **183**: 506-517.
18. LeBoudier E, Rey-Nores JE, Rushmere NK, *et al.* Soluble forms of Toll-like receptor (TLR)2 capable of modulating TLR2 signaling are present in human plasma and breast milk. *J Immunol* 2003; **171**: 6680-6689.
19. Raby AC, Holst B, Le Boudier E, *et al.* Targeting the TLR co-receptor CD14 with TLR2-derived peptides modulates immune responses to pathogens. *Science translational medicine* 2013; **5**: 185ra164.
20. Gonzalez-Mateo GT, Loureiro J, Jimenez-Heffernan JA, *et al.* Chronic exposure of mouse peritoneum to peritoneal dialysis fluid: structural and functional alterations of the peritoneal membrane. *Peritoneal dialysis international : journal of the International Society for Peritoneal Dialysis* 2009; **29**: 227-230.
21. Loureiro J, Aguilera A, Selgas R, *et al.* Blocking TGF-beta1 protects the peritoneal membrane from dialysate-induced damage. *Journal of the American Society of Nephrology : JASN* 2011; **22**: 1682-1695.
22. Liappas G, Gonzalez-Mateo GT, Sanchez-Diaz R, *et al.* Immune-Regulatory Molecule CD69 Controls Peritoneal Fibrosis. *Journal of the American Society of Nephrology : JASN* 2016; **27**: 3561-3576.
23. Catalan MP, Esteban J, Subira D, *et al.* Inhibition of caspases improves bacterial clearance in experimental peritonitis. *Peritoneal dialysis international : journal of the International Society for Peritoneal Dialysis* 2003; **23**: 123-126.
24. Hohlbaum AM, Gregory MS, Ju ST, *et al.* Fas ligand engagement of resident peritoneal macrophages in vivo induces apoptosis and the production of neutrophil chemotactic factors. *J Immunol* 2001; **167**: 6217-6224.
25. Giannandrea M, Parks WC. Diverse functions of matrix metalloproteinases during fibrosis. *Disease models & mechanisms* 2014; **7**: 193-203.
26. Aguirre AR, Abensur H. Protective measures against ultrafiltration failure in peritoneal dialysis patients. *Clinics* 2011; **66**: 2151-2157.

27. Aufricht C, Beelen R, Eberl M, *et al.* Biomarker research to improve clinical outcomes of peritoneal dialysis: consensus of the European Training and Research in Peritoneal Dialysis (EuTRiPD) network. *Kidney international* 2017; **92**: 824-835.
28. Usman Mahmood YC, David W. Johnson. Peritoneal Dialysis Solutions. In: Ekart R (ed). *Peritoneal Dialysis solutions. In:Some Special Problems in Peritoneal Dialysis*, 2016.
29. Tao KM, Li XQ, Yang LQ, *et al.* Glutamine supplementation for critically ill adults. *The Cochrane database of systematic reviews* 2014: CD010050.
30. Kratochwill K, Boehm M, Herzog R, *et al.* Alanyl-glutamine dipeptide restores the cytoprotective stress proteome of mesothelial cells exposed to peritoneal dialysis fluids. *Nephrology, dialysis, transplantation : official publication of the European Dialysis and Transplant Association - European Renal Association* 2012; **27**: 937-946.
31. Ferrantelli E, Liappas G, Vila Cuenca M, *et al.* The dipeptide alanyl-glutamine ameliorates peritoneal fibrosis and attenuates IL-17 dependent pathways during peritoneal dialysis. *Kidney international* 2016; **89**: 625-635.
32. Schmitt CP, Aufricht C. Is there such a thing as biocompatible peritoneal dialysis fluid? *Pediatric nephrology* 2016.
33. Lambie M, Chess J, Donovan KL, *et al.* Independent effects of systemic and peritoneal inflammation on peritoneal dialysis survival. *Journal of the American Society of Nephrology : JASN* 2013; **24**: 2071-2080.
34. Kratochwill K, Lechner M, Lichtenauer AM, *et al.* Interleukin-1 receptor-mediated inflammation impairs the heat shock response of human mesothelial cells. *The American journal of pathology* 2011; **178**: 1544-1555.
35. Bidmon B, Endemann M, Arbeiter K, *et al.* Overexpression of HSP-72 confers cytoprotection in experimental peritoneal dialysis. *Kidney international* 2004; **66**: 2300-2307.
36. Endemann M, Bergmeister H, Bidmon B, *et al.* Evidence for HSP-mediated cytoskeletal stabilization in mesothelial cells during acute experimental peritoneal dialysis. *American journal of physiology Renal physiology* 2007; **292**: F47-56.
37. Joseph C.K. Leung LYC, Kar Neng Lai, Sydney C.W. Tang. Inflammation in Peritoneal Dialysis. In: Peralta AA (ed). *The Latest in Peritoneal Dialysis*, 2013.
38. Kyuden Y, Ito T, Masaki T, *et al.* Tgf-beta1 induced by high glucose is controlled by angiotensin-converting enzyme inhibitor and angiotensin II receptor blocker on cultured human peritoneal mesothelial cells. *Peritoneal dialysis international : journal of the International Society for Peritoneal Dialysis* 2005; **25**: 483-491.

39. Duman S, Gunal AI, Sen S, *et al.* Does enalapril prevent peritoneal fibrosis induced by hypertonic (3.86%) peritoneal dialysis solution? *Peritoneal dialysis international : journal of the International Society for Peritoneal Dialysis* 2001; **21**: 219-224.
40. Margetts PJ, Gyorffy S, Kolb M, *et al.* Antiangiogenic and antifibrotic gene therapy in a chronic infusion model of peritoneal dialysis in rats. *Journal of the American Society of Nephrology : JASN* 2002; **13**: 721-728.
41. Zhang L, Zeng X, Fu P, *et al.* Angiotensin-converting enzyme inhibitors and angiotensin receptor blockers for preserving residual kidney function in peritoneal dialysis patients. *The Cochrane database of systematic reviews* 2014: CD009120.
42. Nongnuch A, Assanatham M, Panorchan K, *et al.* Strategies for preserving residual renal function in peritoneal dialysis patients. *Clinical kidney journal* 2015; **8**: 202-211.
43. Blobe GC, Schiemann WP, Lodish HF. Role of transforming growth factor beta in human disease. *N Engl J Med* 2000; **342**: 1350-1358.
44. Yoshimura A, Wakabayashi Y, Mori T. Cellular and molecular basis for the regulation of inflammation by TGF-beta. *Journal of biochemistry* 2010; **147**: 781-792.
45. Lima CX, Souza DG, Amaral FA, *et al.* Therapeutic Effects of Treatment with Anti-TLR2 and Anti-TLR4 Monoclonal Antibodies in Polymicrobial Sepsis. *PloS one* 2015; **10**: e0132336.
46. Lin CY, Roberts GW, Kift-Morgan A, *et al.* Pathogen-specific local immune fingerprints diagnose bacterial infection in peritoneal dialysis patients. *Journal of the American Society of Nephrology : JASN* 2013; **24**: 2002-2009.
47. Rey Nores JE, Bensussan A, Vita N, *et al.* Soluble CD14 acts as a negative regulator of human T cell activation and function. *Eur J Immunol* 1999; **29**: 265-276.

## FIGURE LEGENDS

**Figure 1. PD solutions (PDS) induce pro-inflammatory and -fibrotic responses in human peritoneal cells.** (a, b) Levels of pro-inflammatory and -fibrotic cytokines in the culture supernatants of (a) non-infected PD effluent-isolated uremic leukocytes and (b) peritoneal mesothelial cells (from omentum) following exposure (16h) to the indicated PDS (1:2 dilution). Results are from one experiment ( $\pm$ SD) representative of 8 (a) and 6 (b) performed with cells from different donors. \* $P$ <0.05; \*\* $P$ <0.01; \*\*\* $P$ <0.005 (PDS vs control). (c, d) Scatter plots show the effect of Dianeal/low (1.36% glucose Dianeal) on the expression of inflammation and immunity-related genes, as assessed by quantitative RT-PCR on RNA extracted from peritoneal leukocytes (c) and peritoneal mesothelial cells (d) following a 16h stimulation. Dotted lines indicate the 0.5 and 2 fold change thresholds.

**Figure 2. TLR2 and TLR4 are involved in PDS-induced pro-inflammatory and -fibrotic responses of peritoneal cells.** Levels of pro-inflammatory and pro-fibrotic cytokines released by (a and c) non-infected PD effluent-isolated uremic leukocytes (n=3) and (b) human peritoneal mesothelial cells (from omentum, n=3) cultured overnight with or without Dianeal/low (1.36% glucose Dianeal; 1:2 dilution) in the presence of the indicated blocking mAbs or isotype-matched control (5  $\mu$ g/ml). mAb blocking of TLR4 was not tested in HPMC, as they do not express TLR4<sup>3,9</sup>. Cytokine levels were determined by single (a, b) or multiplex (c) ELISA. Results are the mean ( $\pm$ SD) of triplicates after background subtraction (cells cultured in the absence of PDS, but presence of the blocking mAbs or isotype control, typically <30% of the Dianeal/low-induced signal and negligible effect of the mAbs on the background levels). Results in (c) are from one experiment representative of three, performed with cells from different donors. \* $P$ <0.05; \*\* $P$ <0.01; \*\*\* $P$ <0.005 (specific mAb(s) vs isotype control).

**Figure 3. PDS does not contain components capable of inducing direct TLR activation.** (a-c) Non-infected PD effluent-isolated uremic leukocytes were cultured with Dianeal/low (PDS), sterile PD effluent collected from PD patients (1:2 dilution), Pam<sub>3</sub>Cys (250 ng/ml) or LPS (50 ng/ml) for

the indicated times. In **(b)**, stimulation was performed in the presence of the indicated blocking mAbs or isotype-matched control (5  $\mu\text{g/ml}$ ). **(a and b)** Show the extent of ERK phosphorylation in gated macrophages as determined by flow cytometry, and **(c)** shows the levels of I $\kappa$ B- $\alpha$  and  $\alpha$ -tubulin (loading control) in leukocyte lysates detected by Western Blot followed by densitometry scanning. Results are from one experiment representative of three.

**Figure 4. Human peritoneal cell exposure to PDS modulates the release of TLR DAMP ligands.** Levels of TLR DAMP ligands in **(a)** non-infected PD effluents (overnight dwell) collected from PD patients (n=8) or **(b and c)** in culture supernatants from **(b)** non-infected PD effluent-isolated uremic leukocytes and **(c)** human peritoneal mesothelial cells (from omentum) stimulated (16h) or not with Dianeal/low (PDS,1:2 dilution). Results in **(b)** and **(c)** are from one experiment ( $\pm$ SD) representative of 8 **(b)** and 6 **(c)**. \*\* $P < 0.01$ ; \*\*\* $P < 0.005$  (PDS vs No PDS).

**Figure 5. Hsp70 and hyaluronan induce TLR-mediated pro-inflammatory responses to PDS by peritoneal leukocytes.** **(a)** Percentage of phosphorylated ERK (pERK)-positive gated macrophages determined by flow cytometry following stimulation of non-infected PD effluent-isolated uremic leukocytes for the indicated times with Hsp70 (500 ng/ml), low molecular mass HA (LMMHA, ~33 kDa, 100  $\mu\text{g/ml}$ ), medium molecular mass HA (MMMHA, ~289 kDa, 100  $\mu\text{g/ml}$ ), Hsp 60 (500 ng/ml), sterile PD effluent from PD patients (1:2 dilution) or Pam<sub>3</sub>Cys (250 ng/ml). Results are from one experiment representative of three. **(b)** IL-8 levels in the culture supernatants of non-infected PD effluent-isolated uremic leukocytes (6 different donors) stimulated (16h) with Dianeal/low (1:2 dilution) or Pam<sub>3</sub>Cys (250 ng/ml, inset) in the presence or absence of the Hsp70 inhibitor, VER155008 (20  $\mu\text{M}$ ), the specific hyaluronan peptide inhibitor, Pep-1, (250  $\mu\text{g/ml}$ ) or the scrambled peptide control (250  $\mu\text{g/ml}$ ). Right inset shows an inhibition specificity control. Percentages on top of bars indicate the extent of inhibition of each donor's peritoneal leukocyte response to PDS by the indicated inhibitory treatment. \* $P < 0.05$ ; \*\* $P < 0.01$ ; \*\*\* $P < 0.005$  (inhibitor vs control).

**Figure 6. Soluble TLR2 (sTLR2) inhibits PDS-induced pro-inflammatory and pro-fibrotic responses by human peritoneal cells.** Cytokine levels (multiplex ELISA) in the culture supernatants of non-infected PD effluent-isolated uremic leukocytes (n=4) stimulated (16h) with Dianeal/low (1:2 dilution) in the presence or absence of human recombinant sTLR2 (250 ng/ml). \*\* $P < 0.01$ ; \*\*\* $P < 0.005$  (sTLR2 vs No sTLR2).

**Figure 7. Involvement of TLR activating DAMPs, TLR2 and TLR4 in PDS-induced pro-inflammatory and pro-fibrotic responses in mice.** (a) Schematic representation of the mouse model of sterile peritoneal fibrosis induced by continuous exposure to PDS used here and for results shown in Figure 8. Following peritoneal catheter insertion and recovery from the surgery (7 days), mice were instilled twice daily for 40 days with Fresenius Standard glucose solution (PDS) or PBS (more details under Materials and Methods). Peritoneal lavages and peritoneal membrane samples were then collected. (b) Levels of Hsp60, Hsp70 and HA in peritoneal lavages from mice instilled with PDS (n=8) or PBS (n=5) (c) Cytokine levels (multiplex ELISA) in the culture supernatants of peritoneal macrophages from wild type (WT), TLR2-deficient (TLR2<sup>-/-</sup>) or TLR4-deficient (TLR4<sup>-/-</sup>) mice stimulated (16h) with Fresenius Standard solution (PDS) or PBS. Results are the mean of one experiment performed with cells from 3 mice. \* $P < 0.05$ ; \*\* $P < 0.01$ ; \*\*\* $P < 0.005$  (PDS vs PBS).

**Figure 8. Soluble TLR2 inhibits PDS-induced peritoneal fibrosis development *in vivo*.** (a-d) The mouse model of sterile peritoneal fibrosis described in Figure 7 was used here. Mice were instilled twice daily with 2 ml of PBS (n=5) or Fresenius Standard glucose solution (PDS, n=8) for 40 days before sacrifice and sample collection. (a) Histological analysis of the peritoneal membrane was conducted as described under Materials and Methods. Representative fields (x40 magnification) are shown; bar plots show the mean ( $\pm$  SEM) of the sub-mesothelial compact zone (SMC) thickness for each group. (b) Cytokine levels in the peritoneal lavages were measured by multiplex ELISA and (c) peritoneal cell populations were quantified by flow cytometry. Results show the mean ( $\pm$  SEM) for each experimental group. (d) Scatter plots show the effect of PDS on



the expression of fibrosis-related genes in the absence and presence of sTLR2, as assessed by quantitative RT-PCR on RNA extracted from peritoneal membrane samples. Open circles outside the dotted lines correspond to genes modulated in a non-statistically significant manner. \* $P < 0.05$ ; \*\* $P < 0.05$ .

**Table 1. Changes in inflammation and immunity-related gene expression in human uremic peritoneal leukocytes exposed to Dianeal/low.**

Gene symbol	Description	PDS*	
		Fold Change**	p value**
<i>Ccl2</i>	Chemokine (C-C motif) ligand 2	2.20	0.0023
<i>Ccr4</i>	Chemokine (C-C motif) receptor 4	2.14	0.0009
<i>Csf2</i>	Colony stimulating factor 2 (granulocyte-macrophage)	0.49	0.0119
<i>Ifnar1</i>	Interferon (alpha, beta and omega) receptor 1	2.15	0.0001
<i>Ifny</i>	Interferon, gamma	2.35	0.0420
<i>Il1β</i>	Interleukin 1, beta	2.94	0.0001
<i>Cxcl8</i>	Interleukin 8	24.25	0.0001
<i>ItgaM</i>	Integrin, alpha M (complement component 3 receptor 3 subunit)	0.23	0.0001
<i>Mapk1</i>	Mitogen-activated protein kinase 1	2.16	0.0001
<i>Mapk8</i>	Mitogen-activated protein kinase 8	2.20	0.0003
<i>Nlrp3</i>	NLR family, pyrin domain containing 3	0.46	0.0003
<i>Ticam1</i>	Toll-like receptor adaptor molecule 1	2.84	0.0014
<i>Tlr1</i>	Toll-like receptor 1	3.93	0.0006
<i>Tlr2</i>	Toll-like receptor 2	4.34	0.0001
<i>Tlr3</i>	Toll-like receptor 3	3.69	0.0372
<i>Tlr5</i>	Toll-like receptor 5	0.04	0.0185
<i>Tlr6</i>	Toll-like receptor 6	2.03	0.0001
<i>Tlr8</i>	Toll-like receptor 8	0.03	0.0001
<i>Tnf</i>	Tumor necrosis factor	5.16	0.0001
<i>Traf6</i>	TNF receptor-associated factor 6	2.67	0.0028

\*Only statistically significant ( $P < 0.05$ ) PDS-induced  $\leq 0.50$  or  $\geq 2.00$  fold changes were considered.

\*\*Compared to No PDS group.

**Table 2. Changes in inflammation and immunity-related gene expression in human peritoneal mesothelial cells exposed to Dianeal/low.**

Gene symbol	Description	PDS*	
		Fold Change**	p value**
<i>Ccl2</i>	Chemokine (C-C motif) ligand 2	2.56	0.0052
<i>Csf2</i>	Colony stimulating factor 2 (granulocyte-macrophage)	6.34	0.0001
<i>Cxcl10</i>	Interleukin 10	0.46	0.0131
<i>Icam1</i>	Intercellular adhesion molecule 1	4.24	0.0001
<i>Il18</i>	Interleukin 18	0.44	0.0028
<i>Il1α</i>	Interleukin 1, alpha	10.71	0.0001
<i>Il1β</i>	Interleukin 1, beta	11.13	0.0001
<i>Il5</i>	Interleukin 5	4.77	0.0001
<i>Il6</i>	Interleukin 6	4.97	0.0001
<i>Cxcl8</i>	Interleukin 8	40.04	0.0001
<i>Lyz</i>	Lyzosyme	0.39	0.0441
<i>Mx1</i>	Myxovirus (influenza virus) resistance 1	0.45	0.0004
<i>Nlrp3</i>	NLR family, pyrin domain containing 3	0.24	0.0438
<i>Tlr7</i>	Toll-like receptor 7	0.43	0.0023

\*Only statistically significant ( $P < 0.05$ ) PDS-induced  $\leq 0.50$  or  $\geq 2.00$  fold changes were considered.

\*\*Compared to No PDS group.

**Table 3. Changes in fibrosis-related peritoneal gene expression at day 40 in mice instilled daily with PDS or PDS + sTLR2.**

Gene symbol	Description	PDS*		PDS + sTLR2		PDS + sTLR2	
		Fold Change**	p value**	Fold Change**	p value**	sTLR2 Inhibition (%)***	p value***
<i>Bcl2</i>	B-cell leukemia/lymphoma 2	2.01	0.0167	0.52	0.0070	147	0.0045
<i>Bmp7</i>	Bone morphogenetic protein 7	2.04	0.0041	0.94	0.5143	105	0.0035
<i>Cav1</i>	Caveolin 1, caveolae protein	2.27	0.0001	0.97	0.0467	102	0.0001
<i>Ccl11</i>	Chemokine (C-C motif) ligand 11	2.42	0.0001	2.26	0.0078	11	0.3599
<i>Ccl12</i>	Chemokine (C-C motif) ligand 12	8.13	0.0485	2.09	0.2993	85	0.0365
<i>Ccl3</i>	Chemokine (C-C motif) ligand 3	25.13	0.0001	4.13	0.0013	87	0.0001
<i>Ccr2</i>	Chemokine (C-C motif) receptor 2	6.14	0.0019	1.08	0.7569	98	0.0020
<i>Col3a1</i>	Collagen, type III, alpha 1	3.07	0.0001	0.67	0.0049	116	0.0000
<i>Cxcr4</i>	Chemokine (C-X-C motif) receptor 4	5.52	0.0001	0.91	0.6275	102	0.0001
<i>Fasl</i>	Fas ligand (TNF superfamily, member 6)	57.50	0.0001	3.59	0.1695	95	0.0001
<i>Hgf</i>	Hepatocyte growth factor	6.18	0.0008	1.72	0.1965	86	0.0031
<i>Ifng</i>	Interferon gamma	20.85	0.0028	4.73	0.0895	81	0.0096
<i>Il10</i>	Interleukin 10	13.81	0.0090	3.51	0.1299	80	0.0020
<i>Il1b</i>	Interleukin 1 beta	26.54	0.0001	1.71	0.0302	97	0.0001
<i>Il4</i>	Interleukin 4	8.47	0.0010	2.24	0.4024	83	0.0004
<i>Itgb3</i>	Integrin alpha 3	3.49	0.0217	0.91	0.2912	103	0.0153
<i>Itgb8</i>	Integrin beta 8	11.11	0.0008	1.09	0.4915	99	0.0009
<i>Lox</i>	Lysyl oxidase	3.01	0.0006	1.07	0.2165	96	0.0008
<i>Mmp14</i>	Matrix metalloproteinase 14 (membrane-inserted)	2.20	0.0023	0.43	0.0108	147	0.0007
<i>Mmp8</i>	Matrix metalloproteinase 8	10.54	0.0001	1.83	0.1712	91	0.0002
<i>Mmp9</i>	Matrix metalloproteinase 9	3.97	0.0001	1.31	0.0105	89	0.0001
<i>Stat1</i>	Signal transducer and activator of transcription 1	7.55	0.0012	1.53	0.0138	92	0.0015
<i>Tgfb1</i>	Transforming growth factor, beta 1	4.04	0.0001	1.39	0.0661	87	0.0003
<i>Tgfb2</i>	Transforming growth factor, beta receptor II	2.33	0.0002	0.91	0.6121	107	0.0006
<i>Timp1</i>	Tissue inhibitor of metalloproteinase 1	26.88	0.0019	1.50	0.0414	98	0.0021
<i>Timp2</i>	Tissue inhibitor of metalloproteinase 2	2.12	0.0001	1.00	0.9520	100	0.0001
<i>Timp3</i>	Tissue inhibitor of metalloproteinase 3	2.58	0.0008	1.25	0.0761	84	0.0029
<i>Timp4</i>	Tissue inhibitor of metalloproteinase 4	2.76	0.0005	1.44	0.0205	75	0.1763
<i>Tnf</i>	Tumor necrosis factor	44.83	0.0045	1.27	0.1213	99	0.0047

\*Only statistically significant ( $P < 0.05$ ) PDS-induced  $\leq 0.5$  or  $\geq 2$  fold changes were considered.

\*\*Compared to PBS group.

\*\*\*Compared to exposure to PDS alone.

**Figure 1**

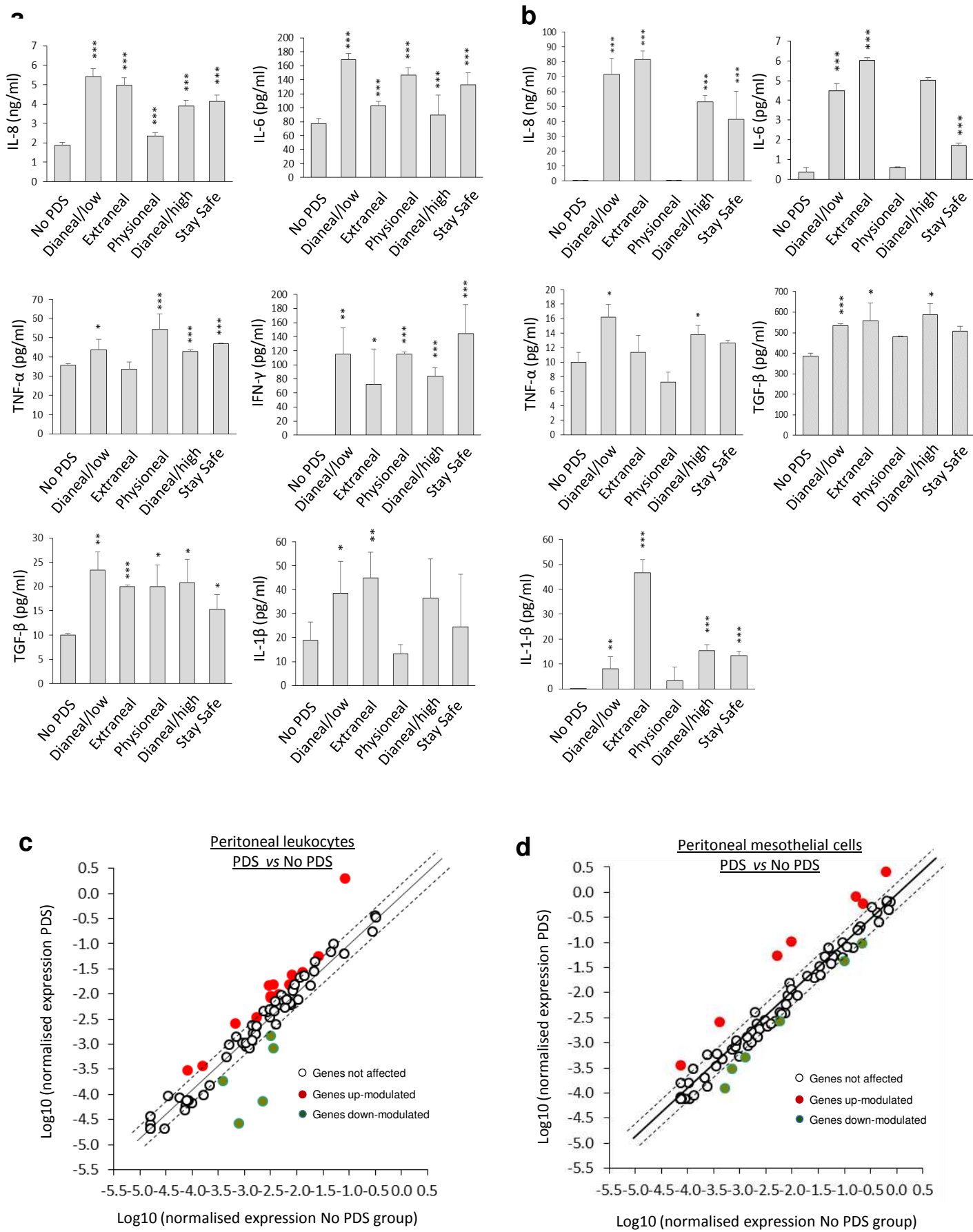
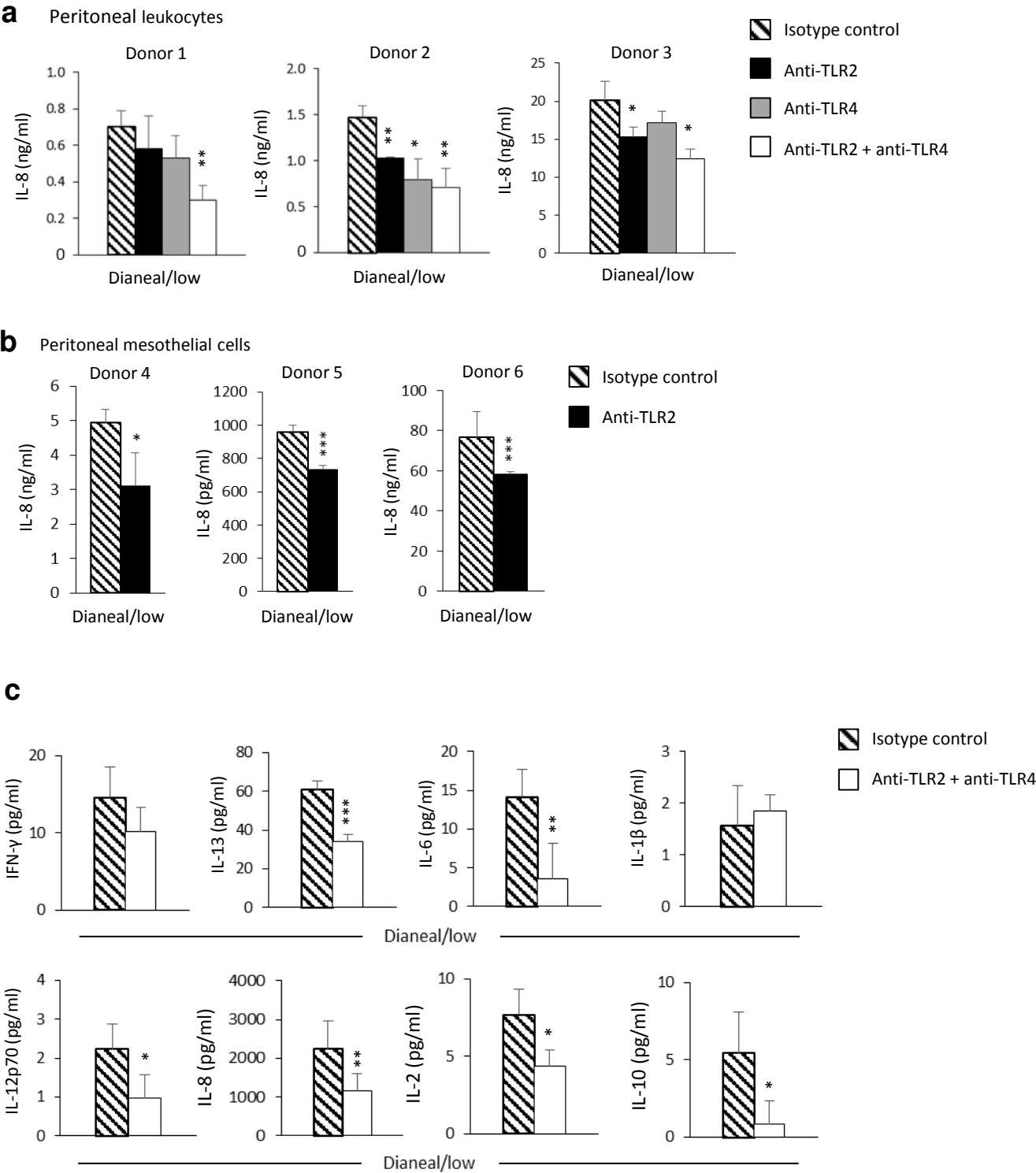
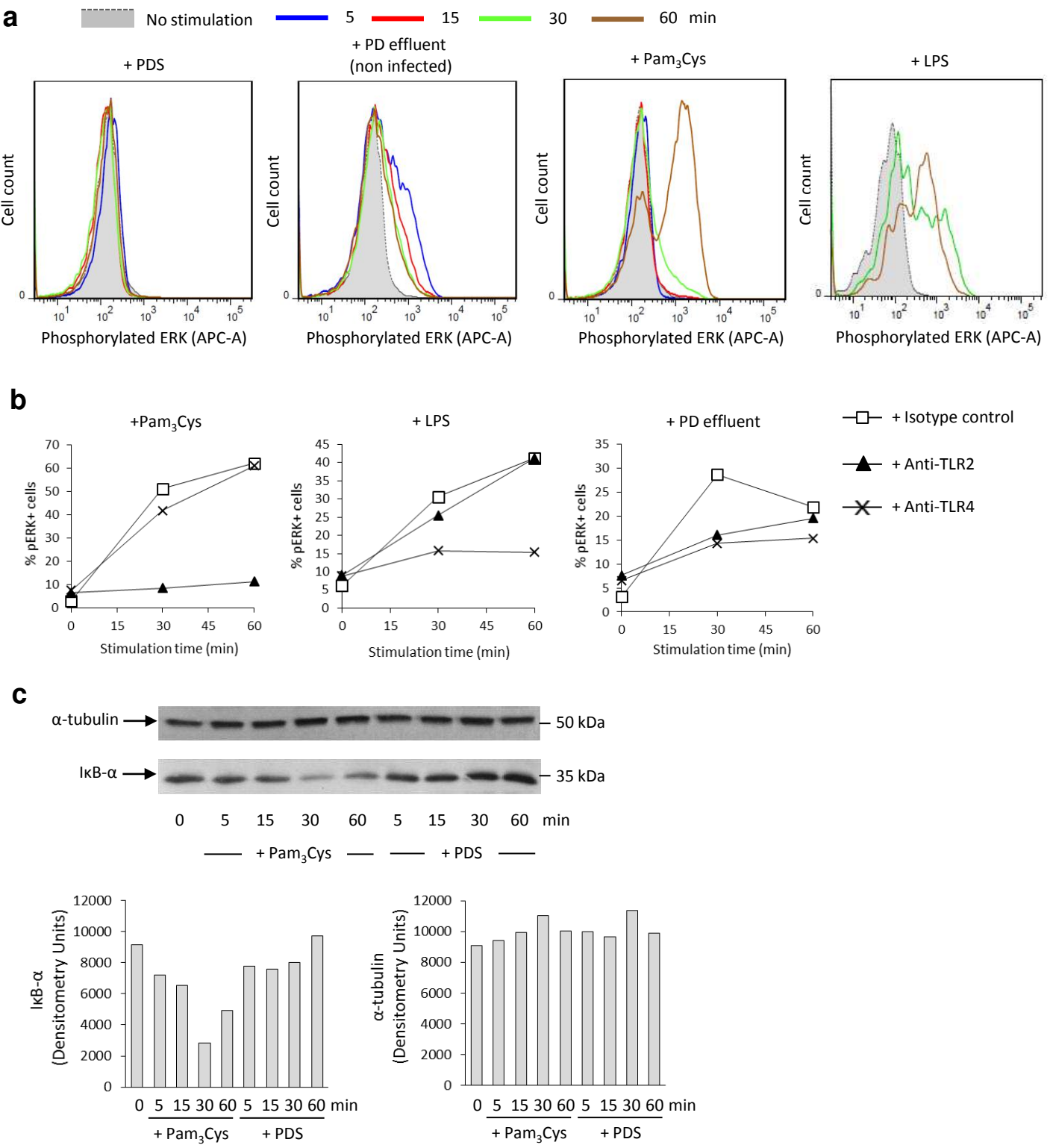


Figure 2



**Figure 3**



**Figure 4**

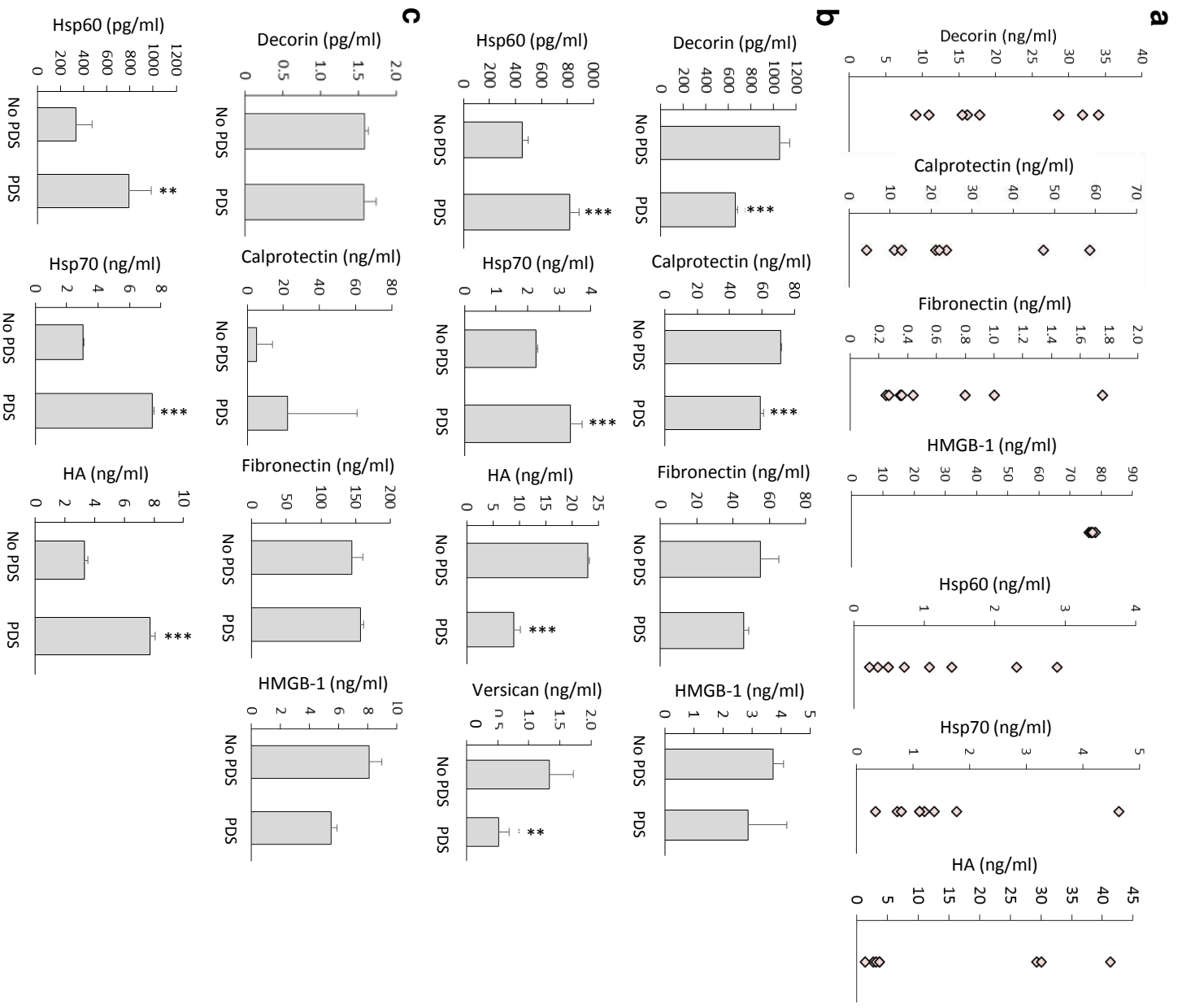
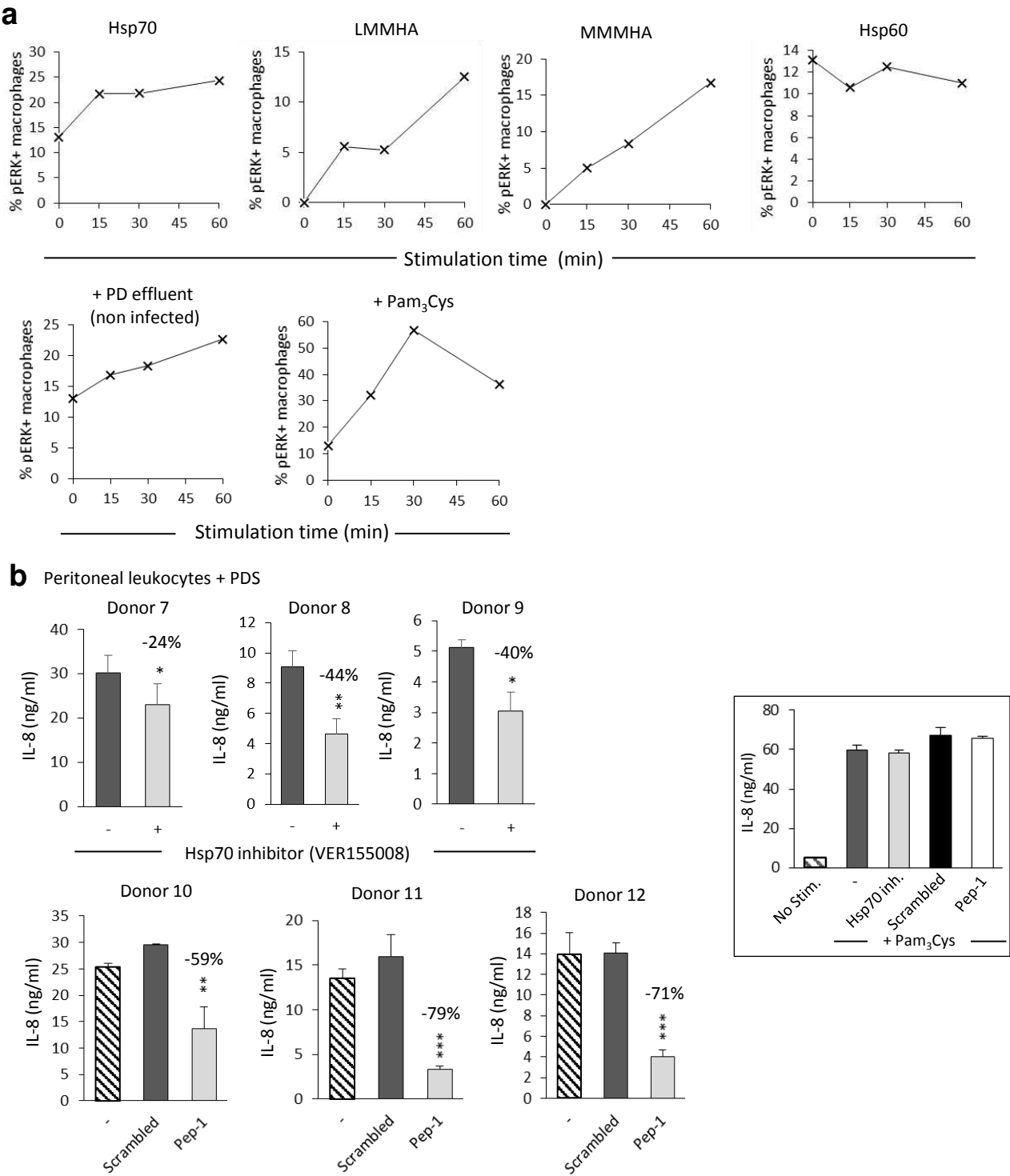


Figure 5





**Figure 6**

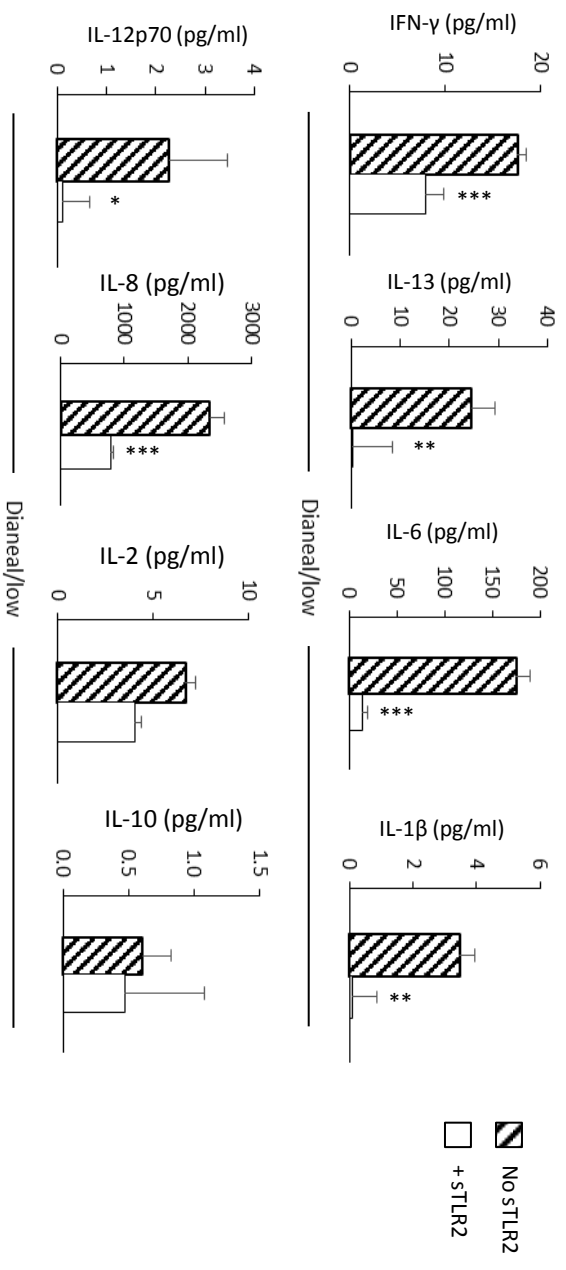
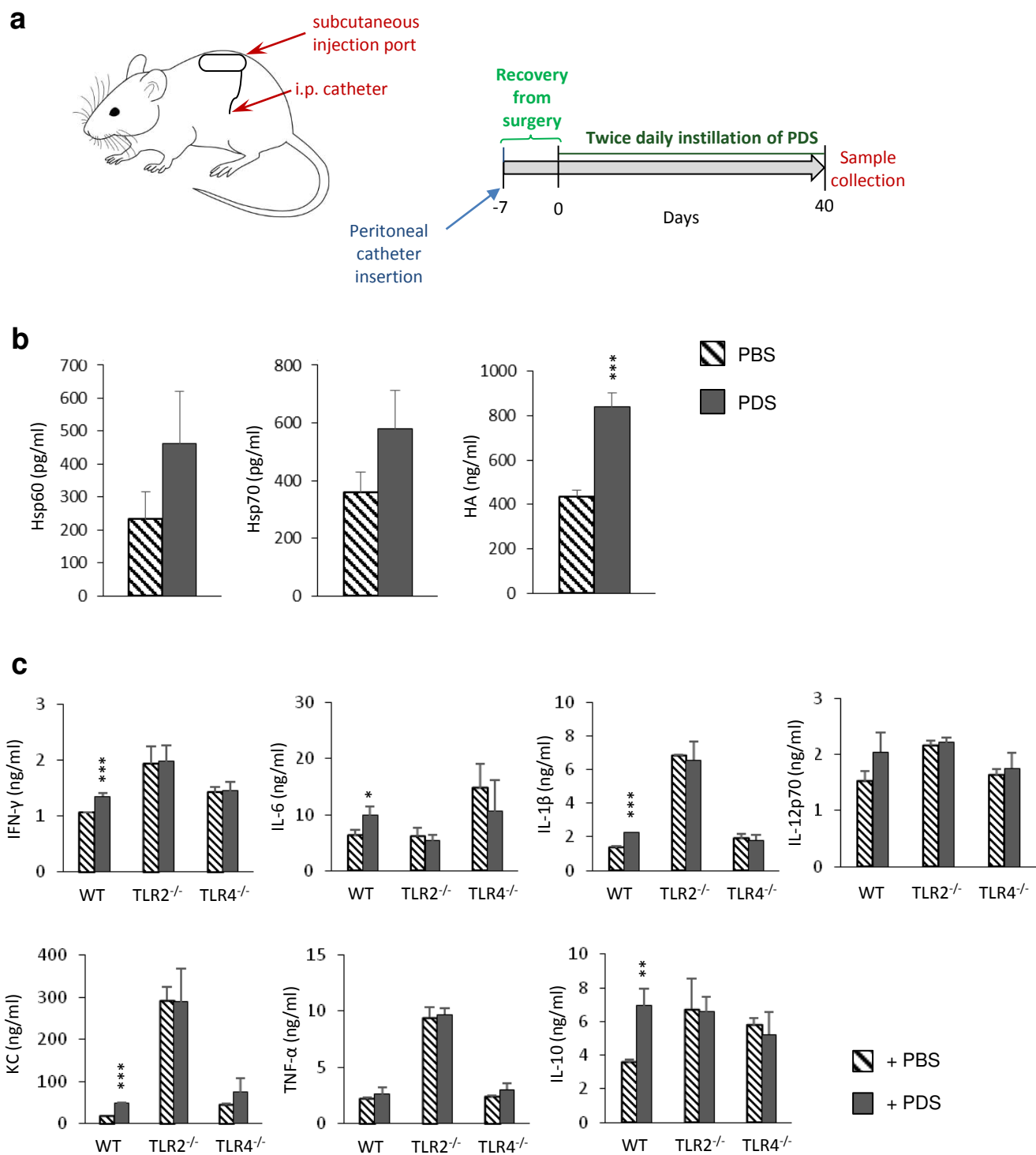
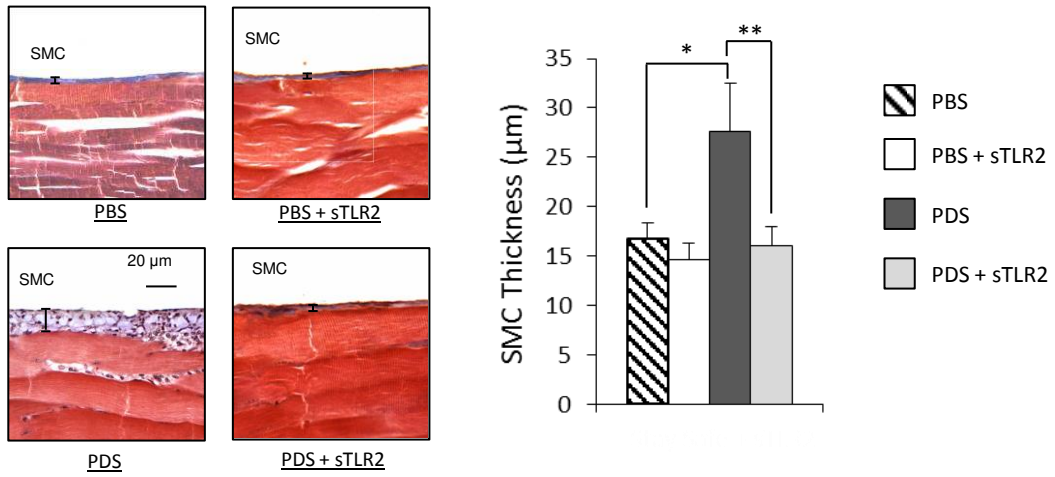
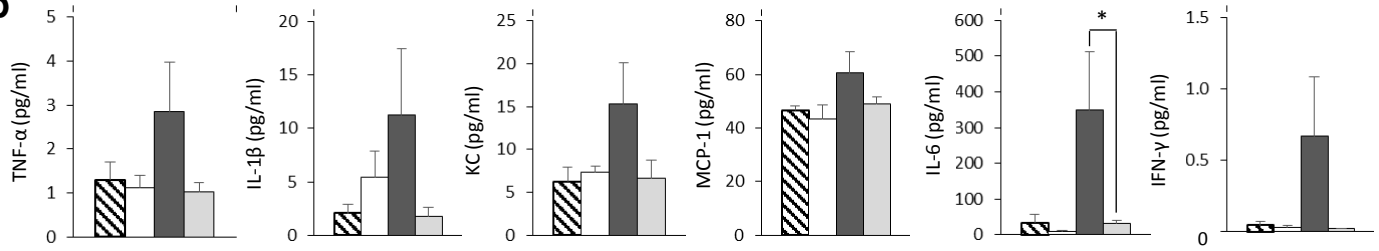
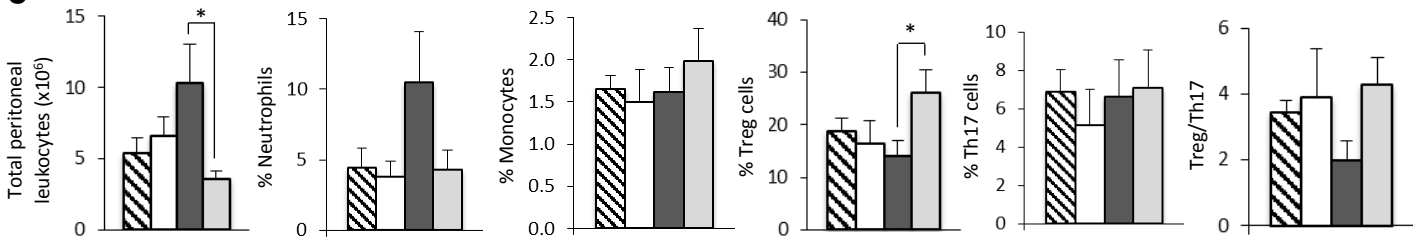
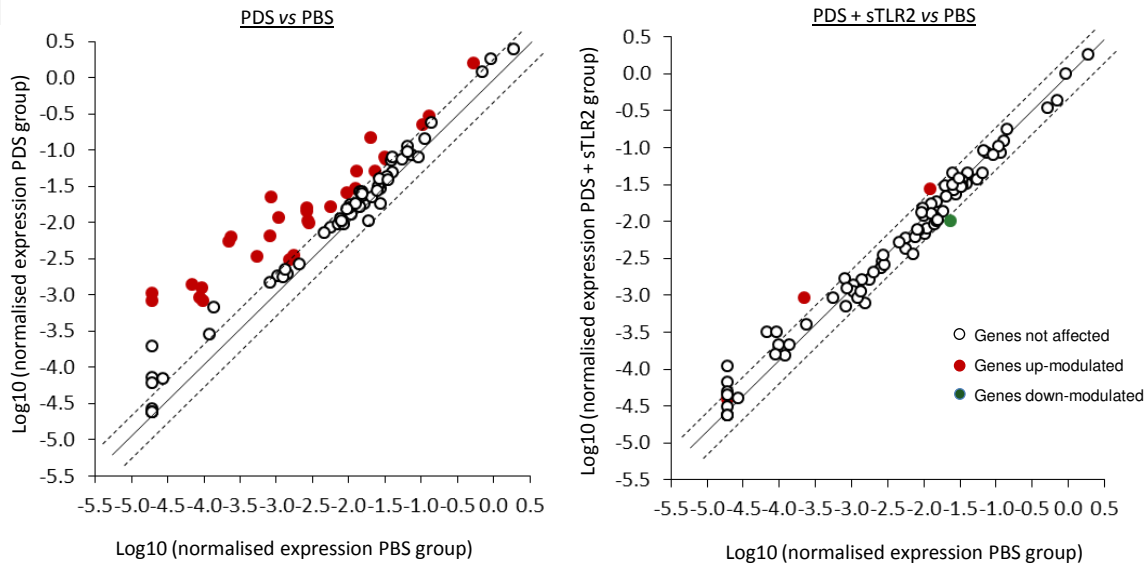
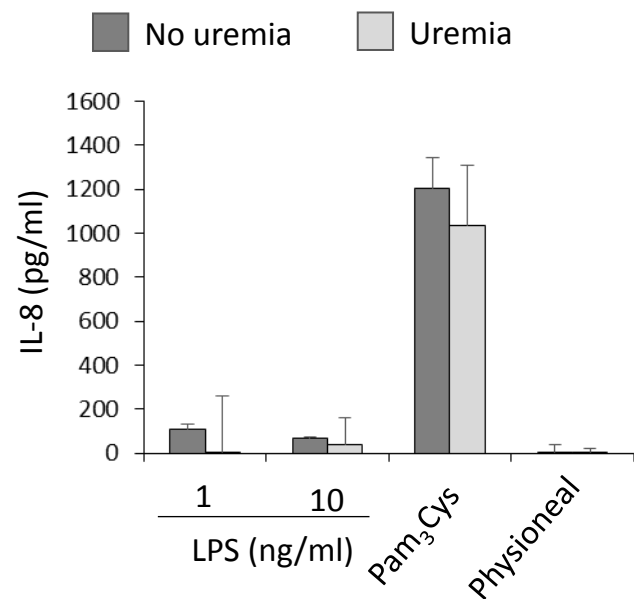


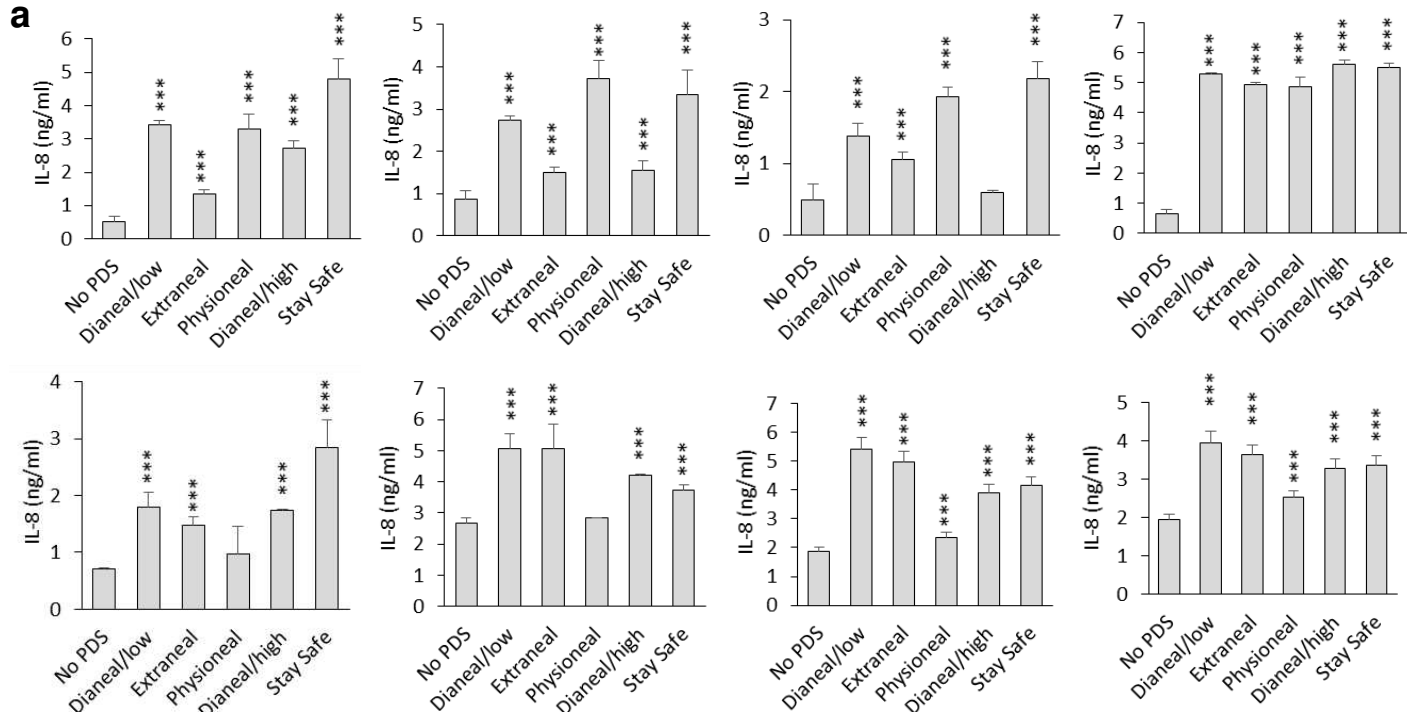
Figure 7



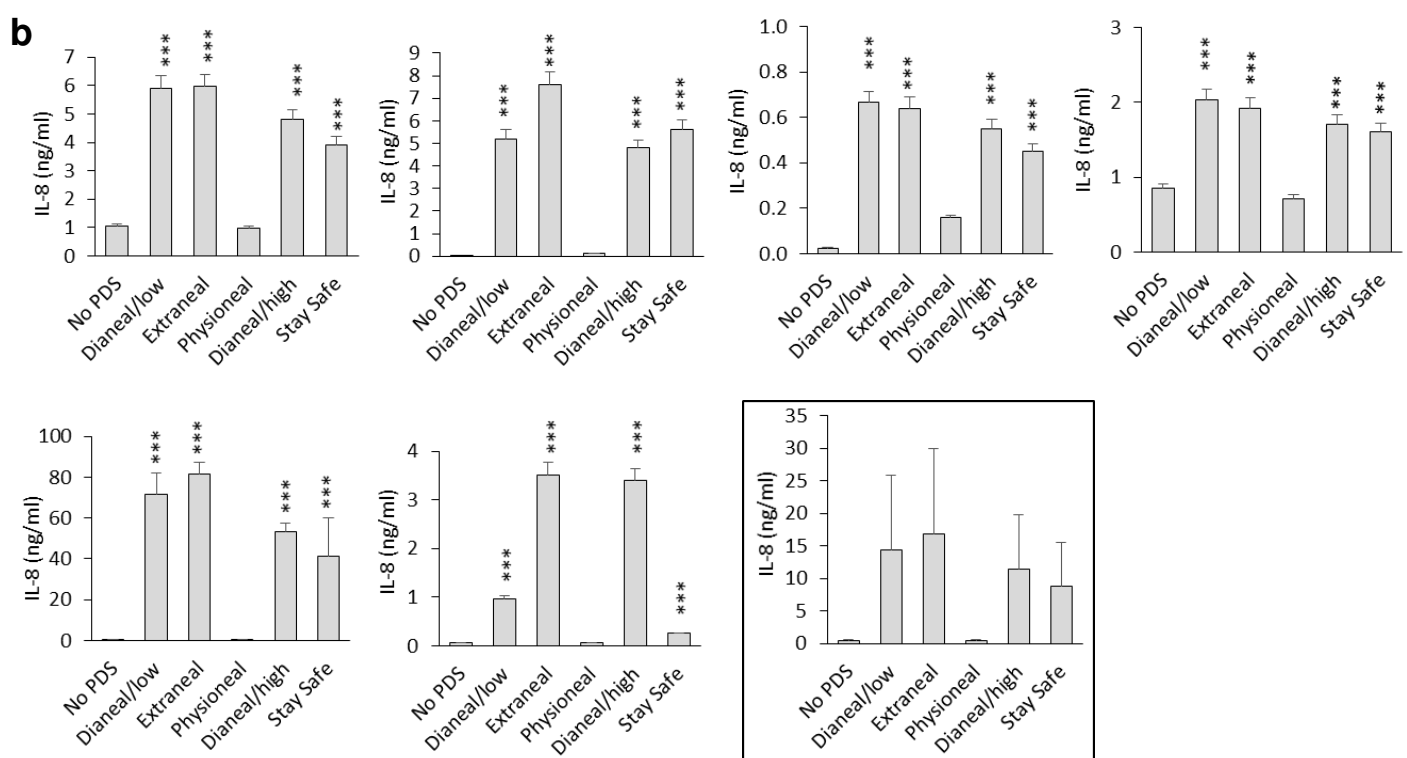
**Figure 8****a****b****c****d**

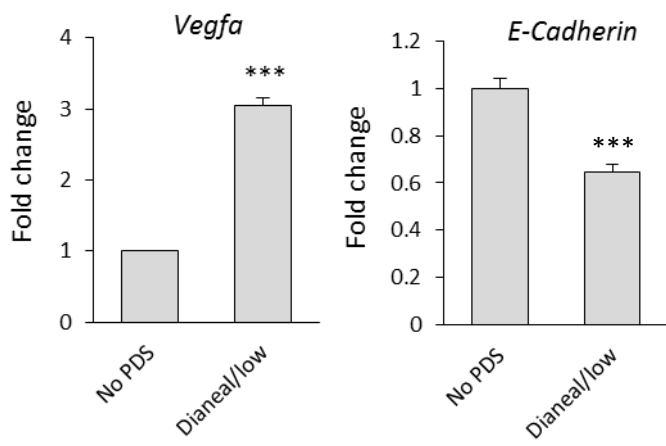


**Supplementary Figure S1. Uremia does not affect the response to TLR2/TLR4 ligands or Physioneal® by mesothelial cells.** Human peritoneal mesothelial cells (from omentum) were exposed (Uremia) or not (No uremia) to uremic PD effluent for 24h. Subsequently, cultures were washed and immediately stimulated (16h) with a TLR4 ligand (LPS, indicated concentrations), a TLR2 ligand (Pam<sub>3</sub>Cys, 100 ng/ml) or Physioneal® (1:2). The histogram plot shows the mean ( $\pm$ SD) IL-8 release after the corresponding background subtraction (exposure or not to PDE) from 1 experiment representative of 3 conducted with mesothelial cells from different donors.

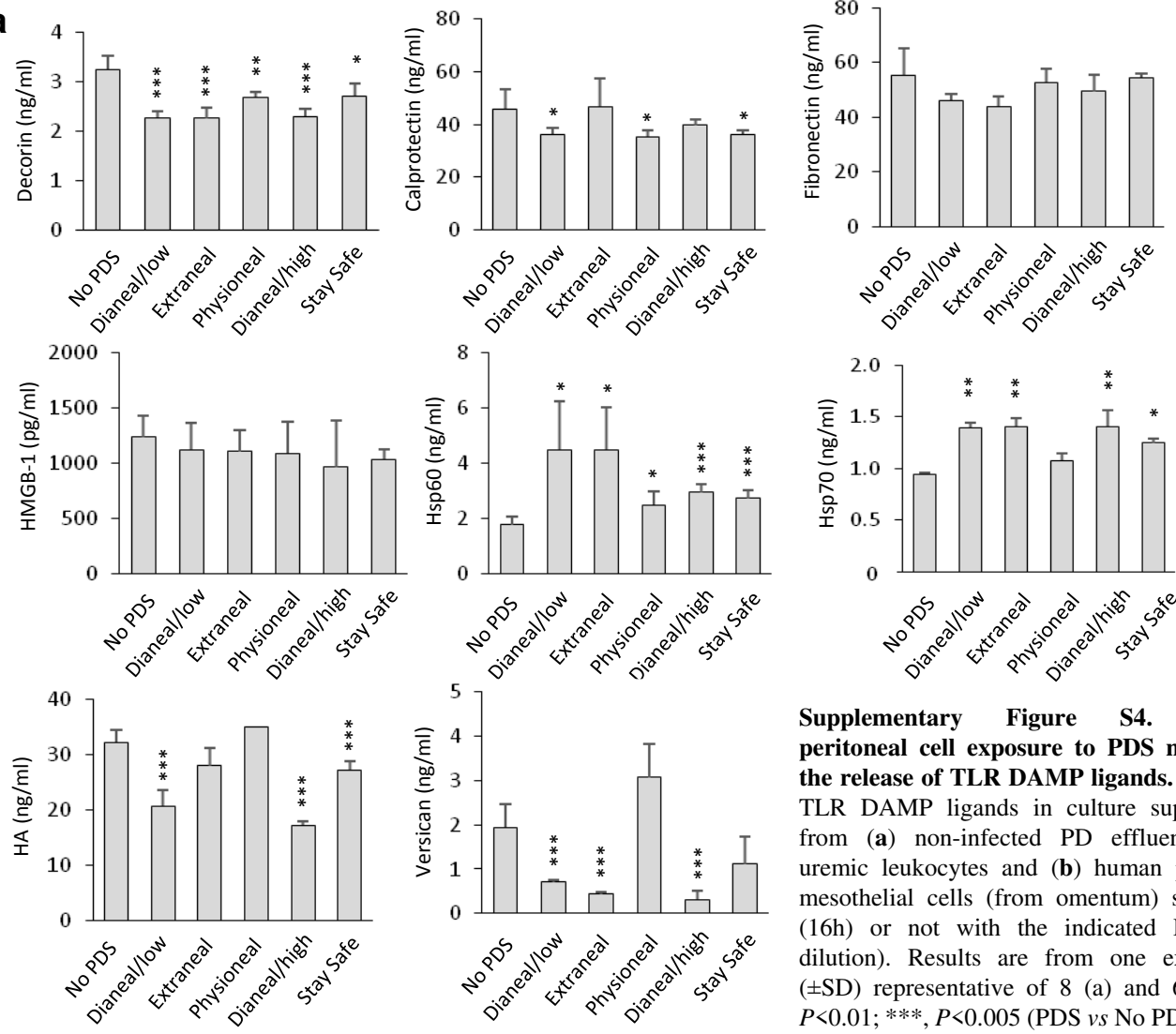
**a**

### Supplementary Figure S2. PD solutions (PDS) induce pro-inflammatory responses in human peritoneal cells. Levels of IL-8 in the culture supernatants of (a) non-infected PD effluent-isolated uremic leukocytes and (b) peritoneal mesothelial cells (from omentum) following exposure (16h) to the indicated PDS (1:2 dilution). Each plot shows the results from one donor run in triplicates ( $\pm$ SD) and the insets show the average of all donors tested ( $\pm$ SEM). \* $P < 0.05$ ; \*\* $P < 0.01$ ; \*\*\* $P < 0.005$ (PDS vs control).

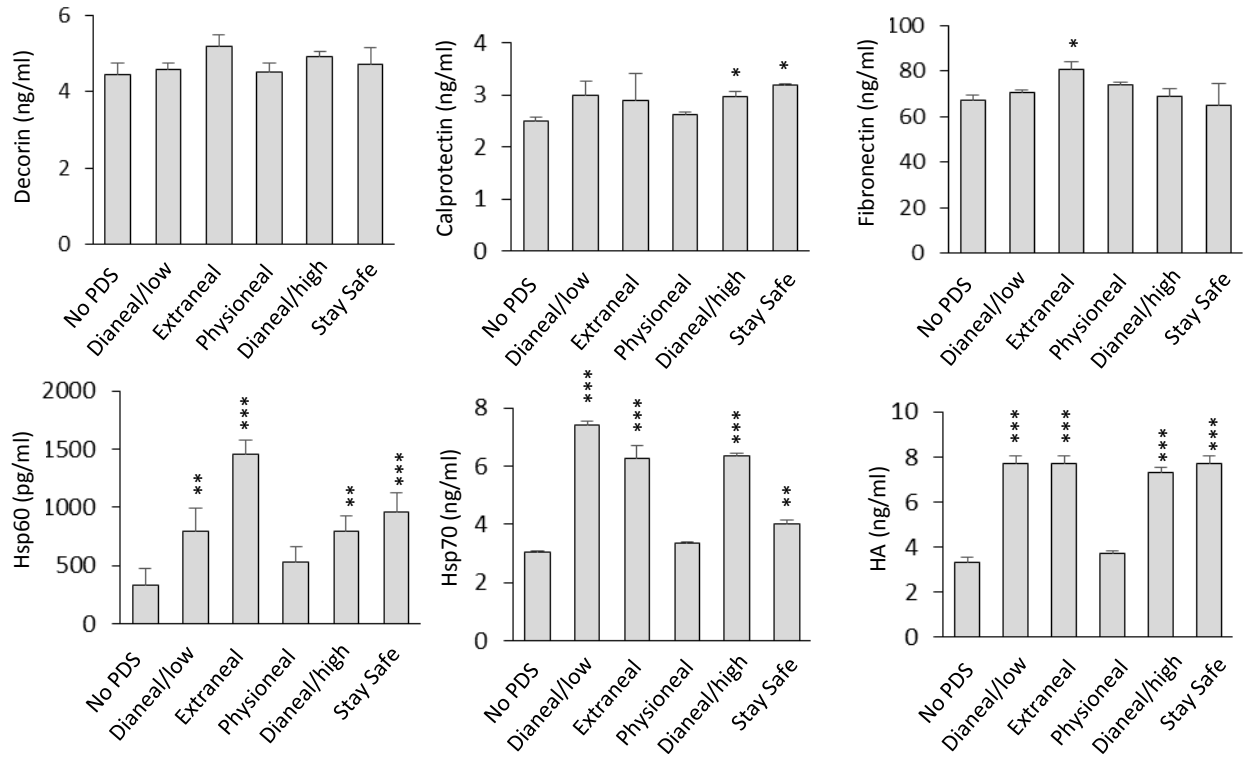
**b**



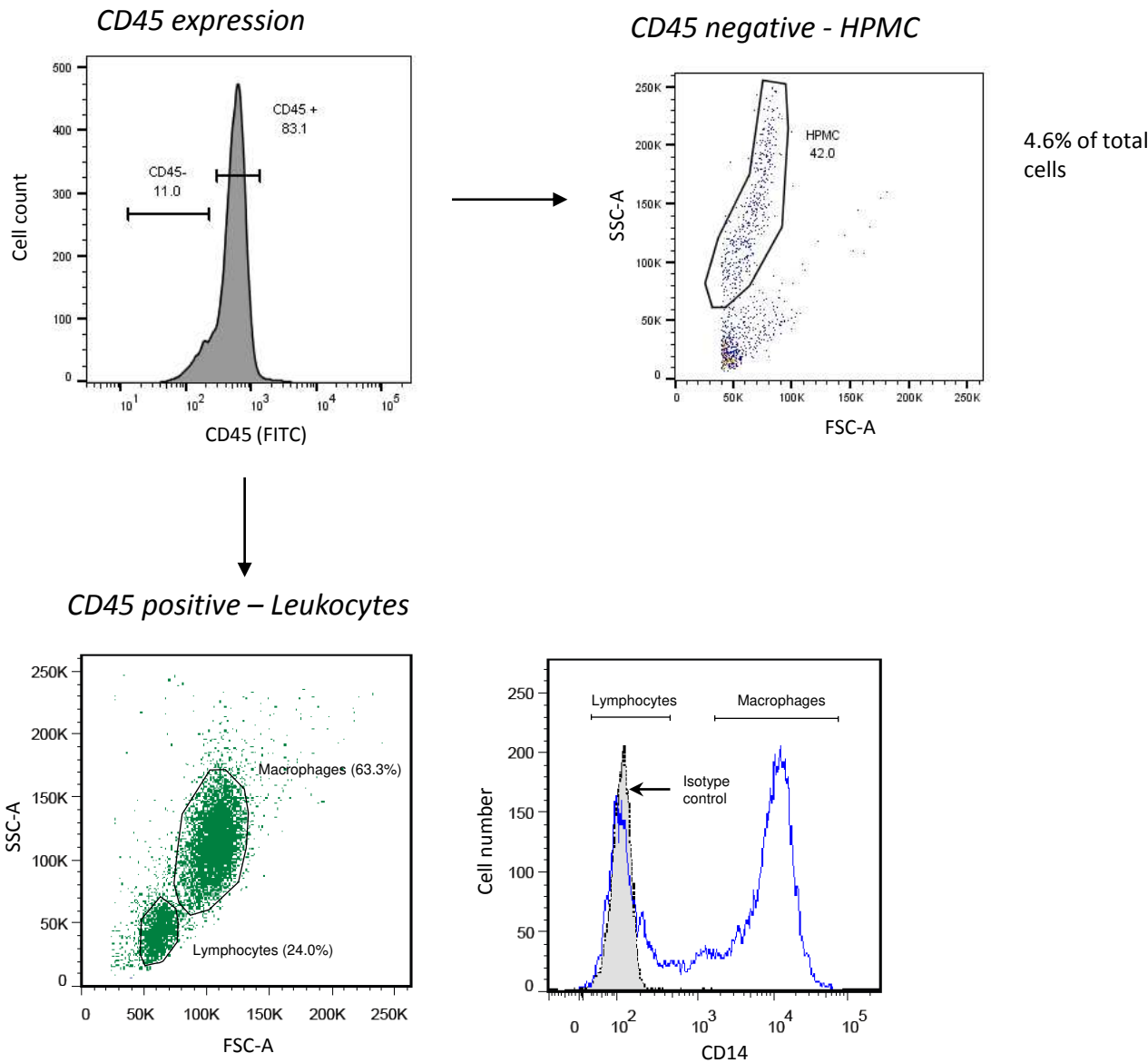
**Supplementary Figure S3. Exposure of human peritoneal mesothelial cells to PDS induces EMT-associated gene expression changes.** Gene expression levels of *Vegfa* and *E-Cadherin* in mesothelial cells (from omentum) were determined by RT-qPCR after 16h culture in the presence or absence of Dianeal/low (1:2 dilution). Histogram plots show the fold change in expression compared to the No PDS control. \*\*\* $P < 0.005$  (Dianeal/low vs No PDS). Results are of one experiment representative of three.

**a**

**Supplementary Figure S4. Human peritoneal cell exposure to PDS modulates the release of TLR DAMP ligands.** Levels of TLR DAMP ligands in culture supernatants from (a) non-infected PD effluent-isolated uremic leukocytes and (b) human peritoneal mesothelial cells (from omentum) stimulated (16h) or not with the indicated PDS (1:2 dilution). Results are from one experiment ( $\pm$ SD) representative of 8 (a) and 6 (b). \*\*,  $P < 0.01$ ; \*\*\*,  $P < 0.005$  (PDS vs No PDS).

**b**

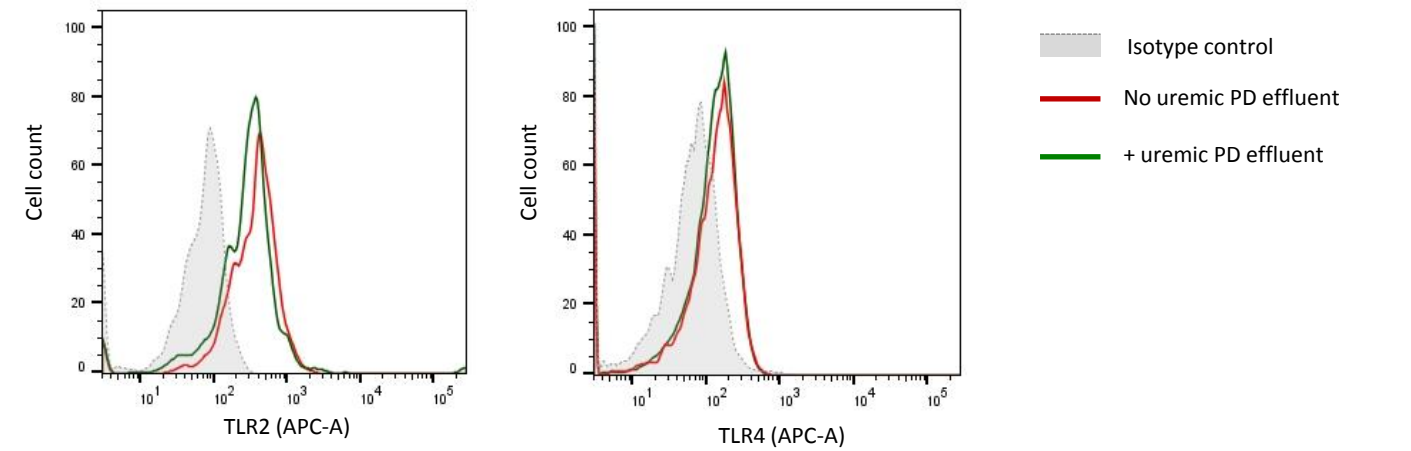
Peritoneal cell composition



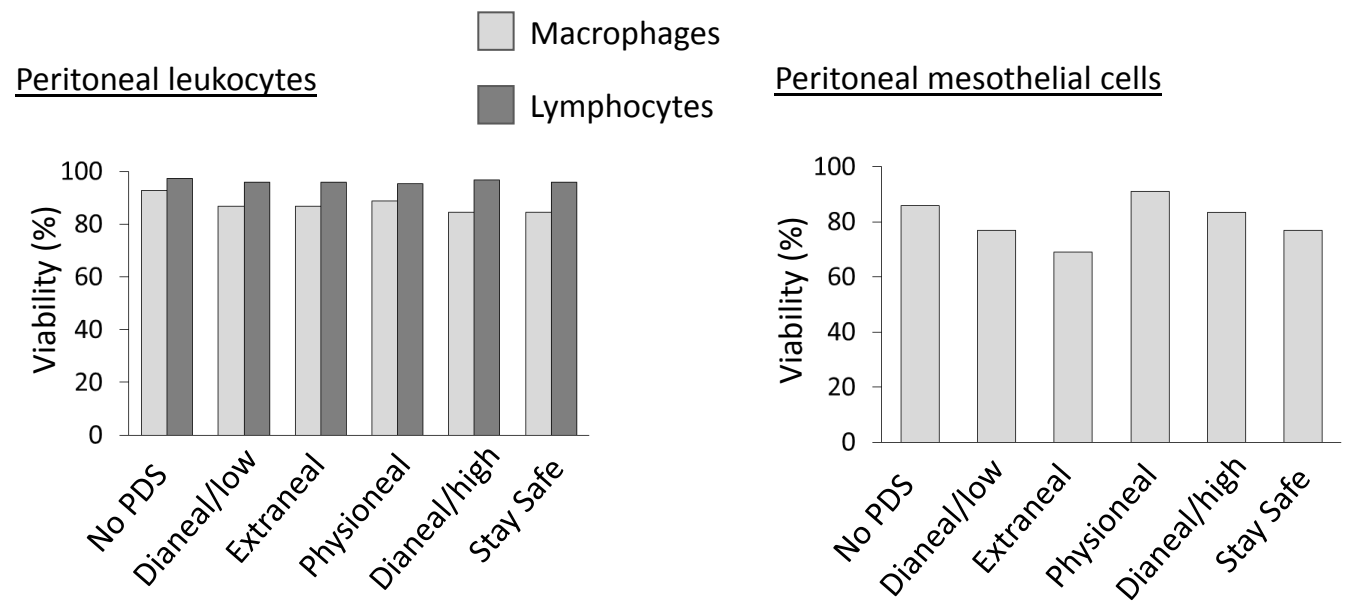
**Supplementary Figure S5. Cellular composition of non-infected PD effluent.** Peritoneal cells were obtained by centrifugation of non-infected PD effluent and stained with CD14- and CD45-specific mAbs prior to flow cytometric analysis. Cell populations were identified on the basis of their forward and side scatter profiles and CD14 and CD45 staining. Mesothelial cells, CD45<sup>-</sup>; leukocytes, CD45<sup>+</sup>; lymphocytes, CD14<sup>-</sup>; monocytes/macrophages, CD14<sup>high</sup>; neutrophils, CD14<sup>low</sup> (typically negligible).



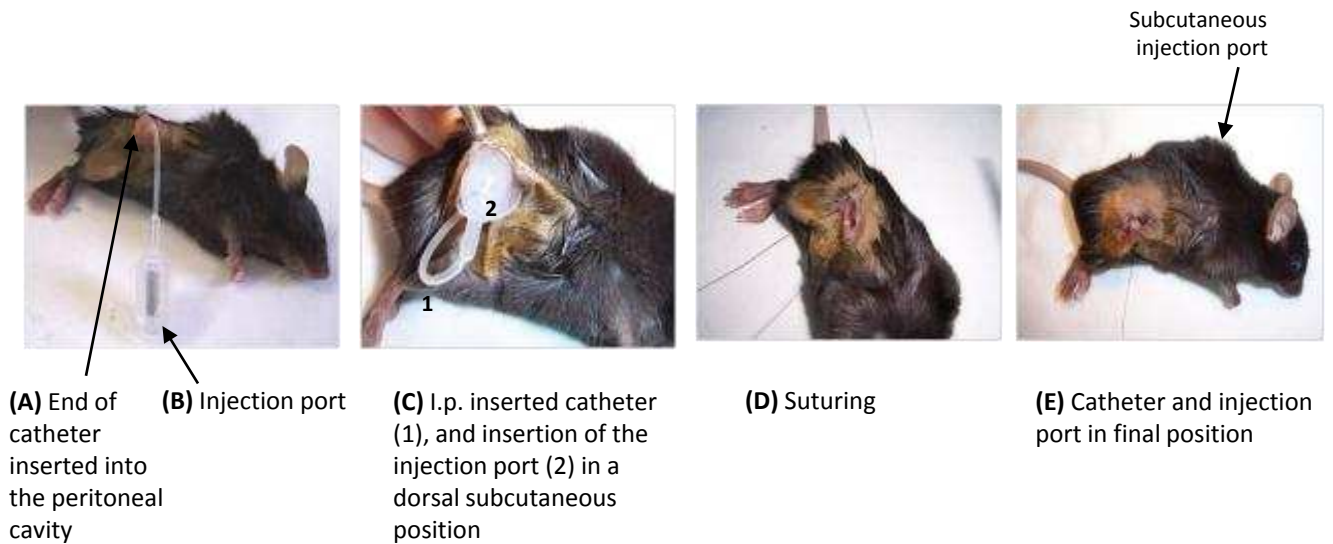
Uremic peritoneal macrophages



**Supplementary Figure S6. Overnight culture in a non-uremic milieu does not affect TLR2/4 expression by uremic macrophages.** Uremic peritoneal leukocytes obtained from PD effluent were incubated (16h) in non-uremic conditions (RPMI), or in uremia-maintaining conditions (RPMI + own PD effluent 1:2). Expression levels of TLR2 (left panel) and TLR4 (right panel) on peritoneal macrophages (gated on the basis of their forward and side scatter profiles and CD14 expression) were determined by flow cytometry. Results are representative of four independent experiments.



**Supplementary Figure S7. Viability of peritoneal cells following overnight exposure to PDS.** Viability of PD effluent-isolated peritoneal leukocytes and peritoneal mesothelial cells (from omentum) following exposure for 16h to the indicated PDS (1:2 dilution). Cell viability was routinely determined by flow cytometry following staining with the viability dye efluor 647.



**Supplementary Figure S8. Surgical procedure of peritoneal catheter insertion in mice.** Inbred 8 to 10-wk-old wild-type female mice (C57/BL6J) underwent surgery under general anaesthesia. Animals were shaved and a large incision was made in the skin on the right flank of the mouse, followed by a small incision of the peritoneal muscle layer, through which the tip of the catheter was inserted into the peritoneal cavity (**A**). The muscle layer was sutured back, ensuring that the catheter would stay in position, and the injection port (**B**) was inserted under the skin in a dorsal position (**C**) before suturing the skin (**D**). The final position of the catheter and injection port is shown in (**E**). One week after surgery, a specially-designed blunt needle was used to pierce the skin and inject the PDS into the catheter through the injection port without damaging it.

**Supplementary Table S1.** Characteristics of the peritoneal dialysis solutions used

PD solution	Manufacturer	pH	Osmotic agent	Osmotic agent concentration	Buffer
Dianeal PD4 1.36%	Baxter	5.5	Glucose	1.36%	Lactate
Dianeal PD4 2.27%	Baxter	5.5	Glucose	2.27%	Lactate
Stay Safe 1.5%	Fresenius	5.5	Glucose	1.5%	Lactate
Stay Safe 4.25% *	Fresenius	5.5	Glucose	4.25%	Lactate
Extraneal	Baxter	5.5	Icodextrin	7.5%	Lactate
Physioneal	Baxter	7.4	Glucose	1.36%	Lactate/bicarbonate

\* PDS used in the experiments described in Figures 7 and 8.

**Supplementary Table S2.** Effect of Dieneal/low (PDS) on inflammation and immunity-related gene expression by human uremic peritoneal leukocytes (complete gene array).\*

Gene symbol	Description	PDS	
		Fold Change**	P Value**
<i>Apcs</i>	Amyloid P component, serum	1.52	0.0058
<i>C3</i>	Complement component 3	1.09	0.1174
<i>Casp1</i>	Caspase 1, apoptosis-related cysteine peptidase (interleukin 1, beta, convertase)	1.11	0.1513
<i>Ccl2</i>	Chemokine (C-C motif) ligand 2	2.20	0.0023
<i>ccl5</i>	Chemokine (C-C motif) ligand 5	0.78	0.0005
<i>Ccr4</i>	Chemokine (C-C motif) receptor 4	2.14	0.0009
<i>Ccr5</i>	Chemokine (C-C motif) receptor 5	0.73	0.0001
<i>Ccr6</i>	Chemokine (C-C motif) receptor 6	1.16	0.0030
<i>Ccr8</i>	Chemokine (C-C motif) receptor 8	0.70	0.3316
<i>Cd14</i>	CD14 molecule	1.93	0.0001
<i>Cd4</i>	CD4 molecule	0.82	0.0240
<i>Cd40</i>	CD40 molecule, TNF receptor superfamily member 5	0.62	0.0056
<i>Cd40lg</i>	CD40 ligand	1.15	0.0866
<i>Cd80</i>	CD80 molecule	0.70	0.3521
<i>Cd86</i>	CD86 molecule	1.63	0.0733
<i>Cd8a</i>	CD8a molecule	0.80	0.0398
<i>Crp</i>	C-reactive protein, pentraxin-related	830.98***	0.3739
<i>Csf2</i>	Colony stimulating factor 2 (granulocyte-macrophage)	0.49	0.0119
<i>Cxcl10</i>	Chemokine (C-X-C motif) ligand 10	63.62***	0.3739
<i>Cxcr3</i>	Chemokine (C-X-C motif) receptor 3	0.86	0.1522
<i>Ddx58</i>	DEAD (Asp-Glu-Ala-Asp) box polypeptide 58	1.30	0.0025
<i>Faslg</i>	Fas ligand (TNF superfamily, member 6)	1.90	0.0117
<i>Foxp3</i>	Forkhead box P3	1.13	0.3339
<i>Gata3</i>	GATA binding protein 3	1.00	0.9585
<i>Hla-A</i>	Major histocompatibility complex, class I, A	1.18	0.0063
<i>Hla-E</i>	Major histocompatibility complex, class I, E	1.05	0.2719
<i>Icam1</i>	Intercellular adhesion molecule 1	1.70	0.0001
<i>Ifna1</i>	Interferon, alpha 1	1.31	0.0001
<i>Ifnar1</i>	Interferon (alpha, beta and omega) receptor 1	2.15	0.0001
<i>Ifnb1</i>	Interferon, beta 1, fibroblast	583.85***	0.3739
<i>Ifng</i>	Interferon, gamma	2.35	0.0420
<i>Ifngr1</i>	Interferon gamma receptor 1	1.87	0.0001
<i>Il10</i>	Interleukin 10	0.80	0.8484
<i>Il13</i>	Interleukin 13	2.29	0.1312
<i>Il17a</i>	Interleukin 17A	830.98***	0.3739
<i>Il18</i>	Interleukin 18 (interferon-gamma-inducing factor)	0.68	0.3947
<i>Il1a</i>	Interleukin 1, alpha	0.68	0.3221
<i>Il1b</i>	Interleukin 1, beta	2.94	0.0001
<i>Il1r1</i>	Interleukin 1 receptor, type I	1.31	0.4271
<i>Il2</i>	Interleukin 2	0.67	0.6658
<i>Il23a</i>	Interleukin 23, alpha subunit p19	1.14	0.5232
<i>Il4</i>	Interleukin 4	2.78	0.1670
<i>Il5</i>	Interleukin 5 (colony-stimulating factor, eosinophil)	1.52	0.4658
<i>Il6</i>	Interleukin 6 (interferon, beta 2)	0.90	0.0595
<i>Cxcl8</i>	Interleukin 8	24.25	0.0001
<i>Irak1</i>	Interleukin-1 receptor-associated kinase 1	1.85	0.0001
<i>Irf3</i>	Interferon regulatory factor 3	1.65	0.0003
<i>Irf7</i>	Interferon regulatory factor 7	1.71	0.0022
<i>ItgaM</i>	Integrin, alpha M (complement component 3 receptor 3 subunit)	0.23	0.0001
<i>Jak2</i>	Janus kinase 2	0.98	0.7506
<i>Ly96</i>	Lymphocyte antigen 96	1.26	0.0001
<i>Lyz</i>	Lysozyme	0.63	0.0001
<i>Mapk1</i>	Mitogen-activated protein kinase 1	2.16	0.0001
<i>Mapk8</i>	Mitogen-activated protein kinase 8	2.20	0.0003
<i>Mbl2</i>	Mannose-binding lectin (protein C) 2, soluble	1.29	0.0004
<i>Mpo</i>	Myeloperoxidase	1.97	0.0010

<i>Mx1</i>	Myxovirus (influenza virus) resistance 1, interferon-inducible protein p78 (mouse)	0.92	0.4822
<i>Myd88</i>	Myeloid differentiation primary response gene (88)	1.20	0.0532
<i>Nfkb1</i>	Nuclear factor of kappa light polypeptide gene enhancer in B-cells 1	1.55	0.0005
<i>Nfkbia</i>	Nuclear factor of kappa light polypeptide gene enhancer in B-cells inhibitor, alpha	1.58	0.0001
<i>Nlrp3</i>	NLR family, pyrin domain containing 3	0.46	0.0003
<i>Nod1</i>	Nucleotide-binding oligomerization domain containing 1	0.87	0.3762
<i>Nod2</i>	Nucleotide-binding oligomerization domain containing 2	0.87	0.5863
<i>Rag1</i>	Recombination activating gene 1	0.60	0.0089
<i>Rorc</i>	RAR-related orphan receptor C	1.33	0.0899
<i>Slc11a1</i>	Solute carrier family 11 (proton-coupled divalent metal ion transporters), member 1	1.83	0.4652
<i>Stat1</i>	Signal transducer and activator of transcription 1, 91kDa	1.37	0.0168
<i>Stat3</i>	Signal transducer and activator of transcription 3 (acute-phase response factor)	2.00	0.0059
<i>Stat4</i>	Signal transducer and activator of transcription 4	1.35	0.0047
<i>Stat6</i>	Signal transducer and activator of transcription 6, interleukin-4 induced	1.67	0.0001
<i>Tbx21</i>	T-box 21	1.99	0.0007
<i>Ticam1</i>	Toll-like receptor adaptor molecule 1	2.84	0.0014
<i>Tlr1</i>	Toll-like receptor 1	3.93	0.0006
<i>Tlr2</i>	Toll-like receptor 2	4.34	0.0001
<i>Tlr3</i>	Toll-like receptor 3	3.69	0.0372
<i>Tlr4</i>	Toll-like receptor 4	1.63	0.0013
<i>Tlr5</i>	Toll-like receptor 5	0.04	0.0185
<i>Tlr6</i>	Toll-like receptor 6	2.03	0.0001
<i>Tlr7</i>	Toll-like receptor 7	0.98	0.6832
<i>Tlr8</i>	Toll-like receptor 8	0.03	0.0001
<i>Tlr9</i>	Toll-like receptor 9	1.25	0.1429
<i>Tnf</i>	Tumor necrosis factor	5.16	0.0001
<i>Traf6</i>	TNF receptor-associated factor 6	2.67	0.0028
<i>Tyk2</i>	Tyrosine kinase 2	1.23	0.0124

\* Statistically significant ( $P < 0.05$ ) and biologically relevant ( $\leq 0.5$ , bold green;  $\geq 2$ , bold red) PDS-induced fold changes are analysed in Results, Table 1.

\*\* Compared to No PDS group.

\*\*\* These transcripts were excluded from Figure 1C, as their Cts were below the detection limits.

**Supplementary Table S3.** Effect of Dieneal/low (PDS) on inflammation and immunity-related gene expression by human peritoneal mesothelial cells (complete gene array).\*

Gene symbol	Description	PDS	
		Fold Change**	P Value**
<i>Apcs</i>	Amyloid P component, serum	1.03	0.3791
<i>C3</i>	Complement component 3	0.97	0.7335
<i>Casp1</i>	Caspase 1, apoptosis-related cysteine peptidase (interleukin 1, beta, convertase)	0.82	0.0004
<i>Ccl2</i>	Chemokine (C-C motif) ligand 2	2.56	0.0052
<i>ccl5</i>	Chemokine (C-C motif) ligand 5	0.57	0.0405
<i>Ccr4</i>	Chemokine (C-C motif) receptor 4	1.02	0.8180
<i>Ccr5</i>	Chemokine (C-C motif) receptor 5	0.99	0.8691
<i>Ccr6</i>	Chemokine (C-C motif) receptor 6	0.71	0.3929
<i>Ccr8</i>	Chemokine (C-C motif) receptor 8	0.68	0.4335
<i>Cd14</i>	CD14 molecule	0.54	0.0004
<i>Cd4</i>	CD4 molecule	1.16	0.0539
<i>Cd40</i>	CD40 molecule, TNF receptor superfamily member 5	0.99	0.7655
<i>Cd40lg</i>	CD40 ligand	1.22	0.2682
<i>Cd80</i>	CD80 molecule	1.05	0.8617
<i>Cd86</i>	CD86 molecule	1.03	0.3791
<i>Cd8a</i>	CD8a molecule	1.02	0.6862
<i>Crp</i>	C-reactive protein, pentraxin-related	1.08	0.0419
<i>Csf2</i>	Colony stimulating factor 2 (granulocyte-macrophage)	6.34	0.0001
<i>Cxcl10</i>	Chemokine (C-X-C motif) ligand 10	0.46	0.0131
<i>Cxcr3</i>	Chemokine (C-X-C motif) receptor 3	0.93	0.0261
<i>Ddx58</i>	DEAD (Asp-Glu-Ala-Asp) box polypeptide 58	0.52	0.0001
<i>Faslg</i>	Fas ligand (TNF superfamily, member 6)	0.60	0.0006
<i>Foxp3</i>	Forkhead box P3	1.11	0.0509
<i>Gata3</i>	GATA binding protein 3	0.79	0.0214
<i>Hla-A</i>	Major histocompatibility complex, class I, A	0.94	0.2607
<i>Hla-E</i>	Major histocompatibility complex, class I, E	0.86	0.0155
<i>Icam1</i>	Intercellular adhesion molecule 1	4.24	0.0001
<i>Ifna1</i>	Interferon, alpha 1	1.78	0.0061
<i>Ifnar1</i>	Interferon (alpha, beta and omega) receptor 1	1.00	0.9511
<i>Ifnb1</i>	Interferon, beta 1, fibroblast	2.41	0.2846
<i>Ifng</i>	Interferon, gamma	0.86	0.4236
<i>Ifngr1</i>	Interferon gamma receptor 1	1.03	0.6816
<i>Il10</i>	Interleukin 10	0.55	0.0194
<i>Il13</i>	Interleukin 13	0.99	0.8921
<i>Il17a</i>	Interleukin 17A	1.03	0.3791
<i>Il18</i>	Interleukin 18 (interferon-gamma-inducing factor)	0.44	0.0028
<i>Il1a</i>	Interleukin 1, alpha	10.71	0.0001
<i>Il1b</i>	Interleukin 1, beta	11.13	0.0001
<i>Il1r1</i>	Interleukin 1 receptor, type I	1.05	0.1596
<i>Il2</i>	Interleukin 2	1.02	0.5357
<i>Il23a</i>	Interleukin 23, alpha subunit p19	0.64	0.0352
<i>Il4</i>	Interleukin 4	1.55	0.3937
<i>Il5</i>	Interleukin 5 (colony-stimulating factor, eosinophil)	4.77	0.0001
<i>Il6</i>	Interleukin 6 (interferon, beta 2)	4.97	0.0001
<i>Cxcl8</i>	Interleukin 8	40.04	0.0001
<i>Irak1</i>	Interleukin-1 receptor-associated kinase 1	0.98	0.8693
<i>Irf3</i>	Interferon regulatory factor 3	1.09	0.1220
<i>Irf7</i>	Interferon regulatory factor 7	0.73	0.0546
<i>ItgaM</i>	Integrin, alpha M (complement component 3 receptor 3 subunit)	0.61	0.0011
<i>Jak2</i>	Janus kinase 2	0.52	0.0006
<i>Ly96</i>	Lymphocyte antigen 96	0.87	0.0176
<i>Lyz</i>	Lysozyme	0.39	0.0441
<i>Mapk1</i>	Mitogen-activated protein kinase 1	0.93	0.0065
<i>Mapk8</i>	Mitogen-activated protein kinase 8	0.90	0.0943
<i>Mbl2</i>	Mannose-binding lectin (protein C) 2, soluble	1.03	0.3791
<i>Mpo</i>	Myeloperoxidase	1.29	0.0858

<i>Mx1</i>	Myxovirus (influenza virus) resistance 1, interferon-inducible protein p78 (mouse)	<b>0.45</b>	0.0004
<i>Myd88</i>	Myeloid differentiation primary response gene (88)	0.70	0.0019
<i>Nfkb1</i>	Nuclear factor of kappa light polypeptide gene enhancer in B-cells 1	1.24	0.0062
<i>Nfkbia</i>	Nuclear factor of kappa light polypeptide gene enhancer in B-cells inhibitor, alpha	1.55	0.0002
<i>Nlrp3</i>	NLR family, pyrin domain containing 3	<b>0.24</b>	0.0438
<i>Nod1</i>	Nucleotide-binding oligomerization domain containing 1	0.60	0.0046
<i>Nod2</i>	Nucleotide-binding oligomerization domain containing 2	1.65	0.0090
<i>Rag1</i>	Recombination activating gene 1	0.60	0.0704
<i>Rorc</i>	RAR-related orphan receptor C	2.42	0.0911
<i>Slc11a1</i>	Solute carrier family 11 (proton-coupled divalent metal ion transporters), member 1	2.14	0.0880
<i>Stat1</i>	Signal transducer and activator of transcription 1, 91kDa	0.56	0.0001
<i>Stat3</i>	Signal transducer and activator of transcription 3 (acute-phase response factor)	0.64	0.0059
<i>Stat4</i>	Signal transducer and activator of transcription 4	0.62	0.0797
<i>Stat6</i>	Signal transducer and activator of transcription 6, interleukin-4 induced	0.73	0.0030
<i>Tbx21</i>	T-box 21	0.58	0.0126
<i>Ticam1</i>	Toll-like receptor adaptor molecule 1	1.57	0.0116
<i>Tlr1</i>	Toll-like receptor 1	0.80	0.0642
<i>Tlr2</i>	Toll-like receptor 2	1.24	0.1403
<i>Tlr3</i>	Toll-like receptor 3	0.75	0.0153
<i>Tlr4</i>	Toll-like receptor 4	0.70	0.0319
<i>Tlr5</i>	Toll-like receptor 5	0.95	0.7062
<i>Tlr6</i>	Toll-like receptor 6	1.09	0.1873
<i>Tlr7</i>	Toll-like receptor 7	<b>0.43</b>	0.0023
<i>Tlr8</i>	Toll-like receptor 8	1.03	0.3791
<i>Tlr9</i>	Toll-like receptor 9	0.95	0.6628
<i>Tnf</i>	Tumor necrosis factor	2.08	0.0888
<i>Traf6</i>	TNF receptor-associated factor 6	1.04	0.2515
<i>Tyk2</i>	Tyrosine kinase 2	0.65	0.0104

\* Statistically significant ( $P < 0.05$ ) and biologically relevant ( $\leq 0.50$ , bold green;  $\geq 2.00$ , bold red) PDS-induced fold changes are analysed in Results, Table 2.

\*\* Compared to No PDS group.



**Supplementary Table S4.** Effect of sTLR2 on fibrosis-related peritoneal gene expression in mice continuously exposed to PDS for 40 days (complete fibrosis gene array)\*

Gene symbol	Description	PDS		PDS + sTLR2		PBS + sTLR2	
		Fold Change**	P Value**	Fold Change**	P Value**	Fold Change**	P Value**
<i>Acta2</i>	Actin, alpha 2, smooth muscle, aorta	1.35	0.0001	0.98	0.6982	0.72	0.0002
<i>Agt</i>	Angiotensinogen (serpin peptidase inhibitor, clade A, member 8)	1.70	0.0025	0.65	0.2185	0.96	0.9649
<i>Akt1</i>	Thymoma viral proto-oncogene 1	1.87	0.0011	0.85	0.5971	1.00	0.9376
<i>Bcl2</i>	B-cell leukemia/lymphoma 2	2.01	0.0167	0.52	0.0070	1.21	0.4206
<i>Bmp7</i>	Bone morphogenetic protein 7	2.04	0.0041	0.94	0.5143	0.70	0.0041
<i>Cav1</i>	Caveolin 1, caveolae protein	2.27	0.0001	0.97	0.0467	1.25	0.0001
<i>Ccl11</i>	Chemokine (C-C motif) ligand 11	2.42	0.0001	2.26	0.0078	2.60	0.0027
<i>Ccl12</i>	Chemokine (C-C motif) ligand 12	8.13	0.0485	2.09	0.2993	1.08	0.9399
<i>Ccl3</i>	Chemokine (C-C motif) ligand 3	25.13	0.0001	4.13	0.0013	0.44	0.3477
<i>Ccr2</i>	Chemokine (C-C motif) receptor 2	6.14	0.0019	1.08	0.7569	1.68	0.0621
<i>Cebpb</i>	CCAAT/enhancer binding protein (C/EBP), beta	1.15	0.2951	0.86	0.9190	1.39	0.0293
<i>Col1a2</i>	Collagen, type I, alpha 2	1.77	0.0001	0.63	0.0001	1.05	0.5104
<i>Col3a1</i>	Collagen, type III, alpha 1	3.07	0.0001	0.67	0.0049	1.90	0.0003
<i>Ctgf</i>	Connective tissue growth factor	0.57	0.0001	0.73	0.2066	2.27	0.0001
<i>Cxcr4</i>	Chemokine (C-X-C motif) receptor 4	5.52	0.0001	0.91	0.6275	2.04	0.0001
<i>Dcn</i>	Decorin	1.97	0.0001	1.07	0.5290	1.78	0.0001
<i>Edn1</i>	Endothelin 1	1.40	0.1995	1.15	0.0191	1.54	0.0002
<i>Egf</i>	Epidermal growth factor	1.11	0.1765	1.08	0.5749	0.83	0.0398
<i>Eng</i>	Endoglin	1.86	0.0002	0.79	0.1424	1.32	0.0004
<i>Fasl</i>	Fas ligand (TNF superfamily, member 6)	57.50	0.0001	3.59	0.1695	1.25	0.2799
<i>Grem1</i>	Gremlin 1	3.88	0.0918	2.66	0.2253	1.17	0.3519
<i>Hgf</i>	Hepatocyte growth factor	6.18	0.0008	1.72	0.1965	1.54	0.1233
<i>Ifng</i>	Interferon gamma	20.85	0.0028	4.73	0.0895	0.32	0.1279
<i>Il10</i>	Interleukin 10	13.81	0.0090	3.51	0.1299	0.24	0.1229
<i>Il13</i>	Interleukin 13	3.28	0.0836	2.42	0.1917	1.17	0.3519
<i>Il13ra2</i>	Interleukin 13 receptor, alpha 2	1.42	0.0245	2.14	0.0220	1.50	0.0149
<i>Il1a</i>	Interleukin 1 alpha	5.00	0.0559	1.55	0.7881	0.49	0.2222
<i>Il1b</i>	Interleukin 1 beta	26.54	0.0001	1.71	0.0302	0.69	0.1491
<i>Il4</i>	Interleukin 4	8.47	0.0010	2.24	0.4024	2.66	0.2944
<i>Il5</i>	Interleukin 5	2.42	0.4883	1.30	0.8130	0.18	0.1238
<i>Ilk</i>	Integrin linked kinase	1.25	0.1698	1.09	0.2925	1.09	0.0817
<i>Inhbe</i>	Inhibin beta E	1.26	0.0244	1.27	0.1213	1.17	0.3519
<i>Itga1</i>	Integrin alpha 1	1.19	0.3027	0.73	0.0247	0.92	0.6005
<i>Itga2</i>	Integrin alpha 2	1.75	0.1607	1.31	0.3369	1.61	0.0185
<i>Itga3</i>	Integrin alpha 3	1.58	0.0217	0.78	0.2912	1.19	0.2878
<i>Itgav</i>	Integrin alpha V	2.00	0.0098	1.15	0.4113	1.25	0.1851
<i>Itgb1</i>	Integrin beta 1 (fibronectin receptor beta)	1.72	0.0006	1.30	0.0016	1.43	0.0001
<i>Itgb3</i>	Integrin beta 3	3.49	0.0001	0.91	0.5891	1.11	0.5334
<i>Itgb5</i>	Integrin beta 5	1.30	0.0107	1.08	0.6065	1.24	0.0115
<i>Itgb6</i>	Integrin beta 6	1.24	0.0348	1.81	0.0047	0.93	0.5935
<i>Itgb8</i>	Integrin beta 8	11.11	0.0008	1.09	0.4915	1.45	0.2101
<i>Jun</i>	Jun oncogene	1.26	0.0412	0.75	0.0069	1.90	0.0013
<i>Lox</i>	Lysyl oxidase	3.01	0.0006	1.07	0.2165	2.28	0.0002
<i>Ltbp1</i>	Latent transforming growth factor beta binding protein 1	0.67	0.0067	0.85	0.0709	1.43	0.0193
<i>Mmp13</i>	Matrix metalloproteinase 13	10.44	0.1116	5.97	0.1013	3.20	0.0764
<i>Mmp14</i>	Matrix metalloproteinase 14 (membrane-inserted)	2.20	0.0023	0.43	0.0108	0.82	0.2338
<i>Mmp1a</i>	Matrix metalloproteinase 1a (interstitial collagenase)	1.18	0.1877	1.14	0.1777	0.97	0.9760
<i>Mmp2</i>	Matrix metalloproteinase 2	1.37	0.0120	0.70	0.1395	0.96	0.5941
<i>Mmp3</i>	Matrix metalloproteinase 3	1.36	0.0074	0.52	0.0001	1.05	0.5740
<i>Mmp8</i>	Matrix metalloproteinase 8	10.54	0.0001	1.83	0.1712	1.00	0.9650
<i>Mmp9</i>	Matrix metalloproteinase 9	3.97	0.0001	1.31	0.0105	0.86	0.6841
<i>Myc</i>	Myelocytomatosis oncogene	1.61	0.0092	1.16	0.5384	1.43	0.0666
<i>Nfkb1</i>	Nuclear factor of kappa light polypeptide gene enhancer in B-cells	1.58	0.0001	1.03	0.6386	1.15	0.0097
<i>Pdgfa</i>	Platelet derived growth factor, alpha	1.14	0.2020	0.91	0.3141	1.32	0.0757
<i>Pdgfb</i>	Platelet derived growth factor, B polypeptide	1.16	0.0350	0.65	0.1169	0.88	0.0169
<i>Plat</i>	Plasminogen activator, tissue	1.52	0.0109	0.67	0.0218	1.19	0.1442

<i>Plau</i>	Plasminogen activator, urokinase	1.48	0.0352	0.81	0.0544	0.95	0.4442
<i>Plg</i>	Plasminogen	1.26	0.0244	1.65	0.0806	1.17	0.3519
<i>Serpina1a</i>	Serine (or cysteine) peptidase inhibitor, clade A, member 1a	1.26	0.0244	1.27	0.1213	1.17	0.3519
<i>Serpine1</i>	Serine (or cysteine) peptidase inhibitor, clade E, member 1	1.32	0.2383	0.98	0.9831	0.51	0.0060
<i>Serpinh1</i>	Serine (or cysteine) peptidase inhibitor, clade H, member 1	1.72	0.0001	0.71	0.0395	1.08	0.0609
<i>Smad2</i>	MAD homolog 2 (Drosophila)	1.77	0.0055	1.22	0.0577	1.21	0.1645
<i>Smad3</i>	MAD homolog 3 (Drosophila)	1.14	0.1476	0.88	0.6035	0.95	0.5169
<i>Smad4</i>	MAD homolog 4 (Drosophila)	1.44	0.0362	1.41	0.0001	1.30	0.0127
<i>Smad6</i>	MAD homolog 6 (Drosophila)	1.44	0.0493	0.75	0.8606	1.37	0.2312
<i>Smad7</i>	MAD homolog 7 (Drosophila)	1.30	0.0249	1.02	0.7460	1.12	0.1189
<i>Snai1</i>	Snail homolog 1 (Drosophila)	2.54	0.0890	1.50	0.4944	0.89	0.6134
<i>Sp1</i>	Trans-acting transcription factor 1	1.61	0.0019	1.21	0.0688	1.37	0.0033
<i>Stat1</i>	Signal transducer and activator of transcription 1	7.55	0.0012	1.53	0.0138	1.16	0.3066
<i>Stat6</i>	Signal transducer and activator of transcription 6	1.69	0.0009	0.85	0.6429	0.78	0.0539
<i>Tgfb1</i>	Transforming growth factor, beta 1	4.04	0.0001	1.39	0.0661	1.35	0.0437
<i>Tgfb2</i>	Transforming growth factor, beta 2	1.48	0.0046	1.05	0.4255	0.95	0.4302
<i>Tgfb3</i>	Transforming growth factor, beta 3	1.10	0.0001	1.09	0.4448	1.44	0.0024
<i>Tgfb1</i>	Transforming growth factor, beta receptor I	1.64	0.0019	1.59	0.0043	1.28	0.0835
<i>Tgfb2</i>	Transforming growth factor, beta receptor II	2.33	0.0002	0.91	0.6121	1.35	0.0516
<i>Tgif1</i>	TGFB-induced factor homeobox 1	1.79	0.0032	0.88	0.7533	1.55	0.0007
<i>Thbs1</i>	Thrombospondin 1	1.61	0.0021	0.68	0.0190	1.30	0.0016
<i>Thbs2</i>	Thrombospondin 2	1.12	0.4463	1.29	0.0671	1.76	0.0023
<i>Timp1</i>	Tissue inhibitor of metalloproteinase 1	26.88	0.0019	1.50	0.0414	3.75	0.0033
<i>Timp2</i>	Tissue inhibitor of metalloproteinase 2	2.12	0.0001	1.00	0.9520	1.44	0.0092
<i>Timp3</i>	Tissue inhibitor of metalloproteinase 3	2.58	0.0008	1.25	0.0761	1.38	0.0042
<i>Timp4</i>	Tissue inhibitor of metalloproteinase 4	2.76	0.0005	1.44	0.0205	2.76	0.0274
<i>Tnf</i>	Tumor necrosis factor	44.83	0.0045	1.27	0.1213	14.84	0.0048
<i>Vegfa</i>	Vascular endothelial growth factor A	1.43	0.0039	0.90	0.3244	0.90	0.0086

\* Statistically significant ( $P < 0.05$ ) and biologically relevant ( $\geq 2.00$ , bold red) PDS-induced fold changes are analysed in Results, Table 3.

\*\*Compared to PBS group.